Variations in Atlantic surface ocean paleoceanography, 50ø-80øN: A time-slice record of the last 30,000 years

Michael Sarnthein, Eystein Jansen, Mara Weinelt, Maurice Arnold, Jean Claude Duplessy, Helmut Erlenkeuser, Astrid Flatøy, Gro Johannessen, Truls Johannessen, Simon Jung, et al.

PALEOCEANOGRAPHY, VOL. 10, NO. 6, PAGES 1063-1094, DECEMBER 1995

Variations in Atlantic surface ocean paleoceanography, 50°-80°N: A time-slice record of the last 30,000 years

Michael Sarnthein,[1] Eystein Jansen,[2] Mara Weinelt,[1] Maurice Arnold,[3] Jean Claude Duplessy,[3] Helmut Erlenkeuser,[4] Astrid Flatøy,[2] Gro Johannessen,[2] Truls Johannessen,[2] Simon Jung,[1] Nalan Koc,[2] Laurent Labeyrie,[3] Mark Maslin,[1,5] Uwe Pflaumann,[1] and Hartmut Schulz[1,6]

Abstract. Eight time slices of surface-water paleoceanography were reconstructed from stable isotope and paleotemperature data to evaluate late Quaternary changes in density, current directions, and sea-ice cover in the Nordic Seas and NE Atlantic. We used isotopic records from 110 deep-sea cores, 20 of which are accelerator mass spectrometry (AMS)-^{14}C dated and 30 of which have high (>8 cm /kyr) sedimentation rates, enabling a resolution of about 120 years. Paleotemperature estimates are based on species counts of planktonic foraminifera in 18 cores. The $\delta^{18}O$ and $\delta^{13}C$ distributions depict three main modes of surface circulation: (1) The Holocene-style interglacial mode which largely persisted over the last 12.8 ^{14}C ka, and probably during large parts of stage 3. (2) The peak glacial mode showing a cyclonic gyre in the, at least, seasonally ice-free Nordic Seas and a meltwater lens west of Ireland. Based on geostrophic forcing, it possibly turned clockwise, blocked the S-N flow across the eastern Iceland-Shetland ridge, and enhanced the Irminger current around west Iceland. It remains unclear whether surface-water density was sufficient for deepwater formation west of Norway. (3) A meltwater regime culminating during early glacial Termination I, when a great meltwater lens off northern Norway probably induced a clockwise circulation reaching south up to Faeroe, the northward inflow of Irminger Current water dominated the Icelandic Sea, and deepwater convection was stopped. In contrast to circulation modes two and three, the Holocene-style circulation mode appears most stable, even unaffected by major meltwater pools originating from the Scandinavian ice sheet, such as during $\delta^{18}O$ event 3.1 and the Bölling. Meltwater phases markedly influenced the European continental climate by suppressing the "heat pump" of the Atlantic salinity conveyor belt. During the peak glacial, melting icebergs blocked the eastward advection of warm surface water toward Great Britain, thus accelerating buildup of the great European ice sheets; in the early deglacial, meltwater probably induced a southward flow of cold water along Norway, which led to the Oldest Dryas cold spell.

Introduction

The circulation regime in the Nordic Seas has a strong impact on the climate of the adjacent continents. Today, the warm waters of the North Atlantic Drift, the Irminger Current, and the Norwegian Current work as a "heat pump" that provides both heat and moisture to Europe and Iceland; whereas to the west the presence of the Greenland ice sheet is linked to the cold east Greenland Current (Figure 1). In conjunction with cold air masses originating from the Greenland ice cap and the Arctic, the saline surface currents from the south induce strong deepwater formation in the Nordic Seas, which form the most important deepwater source of the global oceanic "salinity conveyor belt" (SCB) [*Stommel*, 1961; *Rooth*, 1982; *Gordon*, 1986]. Past variations in this current system may have resulted in major short-term and long-term changes of climate in the northern hemisphere and, moreover, of the thermohaline circulation in the Atlantic and the global ocean [*Stommel*, 1961; *Emiliani et al.*, 1978; *Broecker*, 1992; *Broecker and Peng*, 1989; *Broecker et al.*, 1985a, b, 1990]. It is essential to add to the understanding of the general and local mechanisms in the northern ocean circulation system which might have triggered the dramatic changes in climate that are observed so frequently over the last glacial-to-interglacial cycle.

Based on more than a hundred age-calibrated planktonic $\delta^{18}O$ and $\delta^{13}C$ records of *Neogloboquadrina pachyderma* (s), this study tries to reconstruct the regional distribution patterns of past surface-water masses in the Nordic Seas, 50°-80°N

[1]Geologisch-Paläontologisches Institut, University of Kiel, Kiel, Germany.
[2]Department of Geology, University of Bergen, Bergen, Norway.
[3]Centre des Faibles Radioactivités, Gif sur Yvette, France.
[4]Leibniz-Labor für Altersbestimmung und Isotopenforschung, University of Kiel, Kiel, Germany.
[5]Also at The Godwin Laboratory, University of Cambridge, Cambridge, England.
[6]Now at Bundesanstalt für Geowissenschaften und Rohstoffe, Hannover, Germany.

Paper number 95PA01453.
0883-8305/95/95PA-01453$10.00

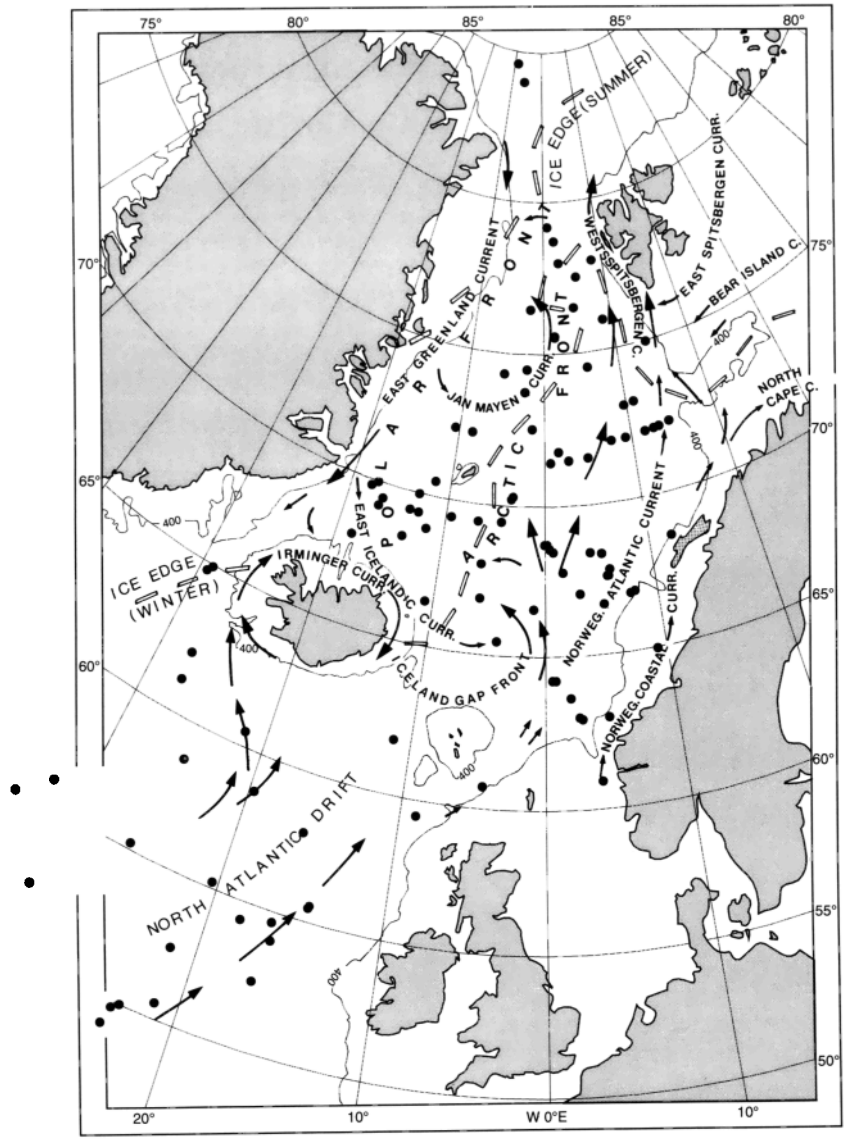

Figure 1. Distribution of modern surface water currents in the Nordic Seas and the northeast North Atlantic [*Hurdle*, 1986; *Dietrich and Ulrich*, 1969]. Circles are core locations. Bars mark ice margins during summer and winter.

(Figure 2). More specifically, it tries to estimate paleoceanographic changes that occurred between the climatic extremes of the Holocene climatic optimum and the last glacial maximum (LGM) and various abrupt, short-term climate excursions at the end of isotope stage 3 and during glacial Termination I. These reconstructions rely on a series of studies of the modern distributions of stable isotopic values in surface waters of the Nordic Seas [*Horwege*, 1986; *Johannessen et al.*, 1994; *Weinelt*, 1993] and in the sea-ice covered Arctic Ocean [*Spielhagen and Erlenkeuser*, 1994].

Our data set which, in addition to many new records, integrates numerous data and ideas of *Keigwin and Boyle* [1989], *Vogelsang* [1990], *Karpuz and Jansen* [1992], *Weinelt* [1993], and many other authors (Table 1), is unique in various ways: (1) it combines evidence from 110 sediment cores from a small key region of the world ocean (Table 1); (2) it contains 21 cores with at least some accelerator mass spectrometry (AMS) ^{14}C dates (Figure 2); and (3) it includes more than 30 cores which provide a high-resolution stratigraphy based on sedimentation rates of more than 7.5-10 cm/1000 years across Termination I (Table 1). Although our grid of coring stations is fairly irregular and large parts of the Lofoten Basin, northern Greenland, and eastern Icelandic Seas still lack any stations, our data set enables us to clearly characterize the extent of all modern surface water masses by multicore records (Figures 1 and 2).

The characteristics of paleowater masses as reflected by the distribution of stable isotopes can be assessed more precisely by linking the isotope data to the various sea surface temperature (SST) and current pattern estimates deduced from planktonic foraminifera [*Kellogg*, 1980; *Schulz*, 1994], U_k^{37} data [*Rosell-Melé*, 1994], and diatom assemblages [*Karpuz and Jansen*, 1992; *Koc et al.*, 1993]. According to *Duplessy et al.* [1991, 1992], oxygen isotopic and SST records can be converted to estimates of paleosalinity within the glacial North Atlantic, which enables us to reconstruct the

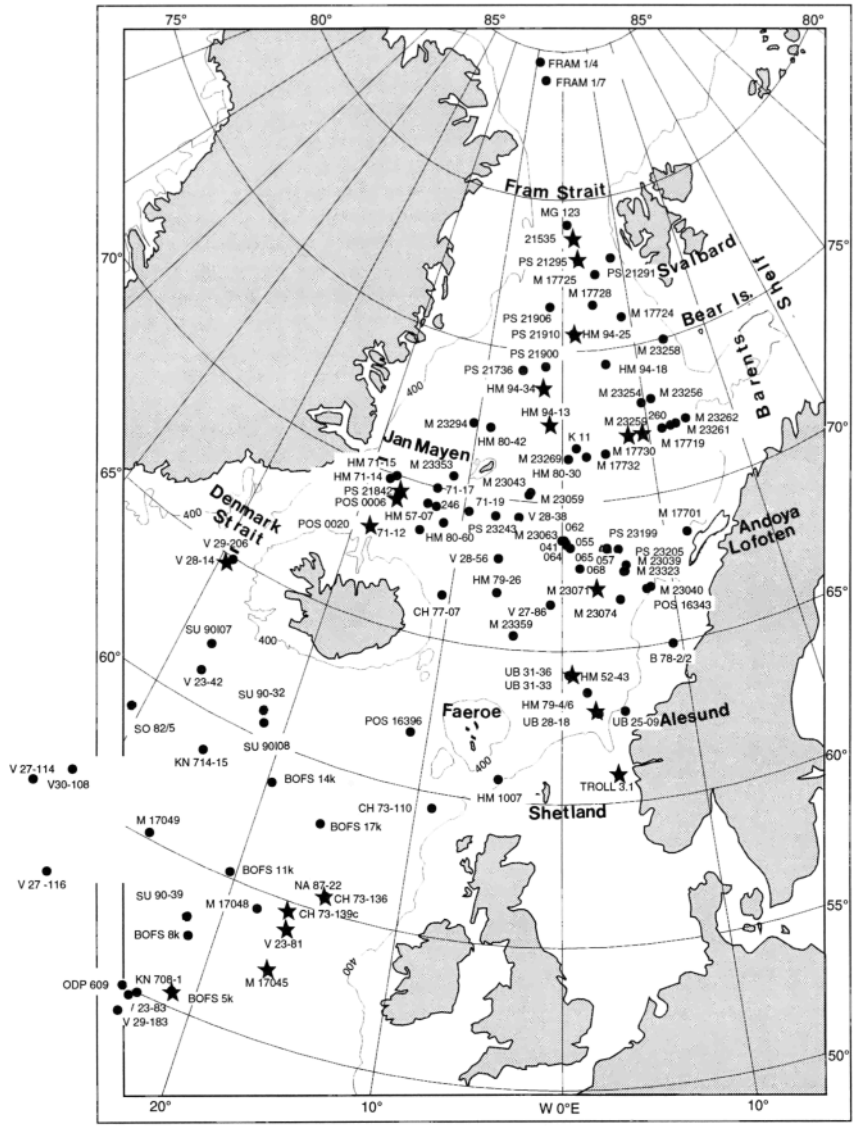

Figure 2. Core locations. Asterisks mark cores with accelerator mass spectrometry (AMS)-^{14}C age control.

Table 1. Core Locations, Sources of Stable Isotope Records, and Sedimentation Rate Estimates for Glacial Termination I

Core	Latitude	Longitude	Water Depth, m	Sedimentation Rate Across Termination I, cm/kyr	DataSource/ Laboratory for $\delta^{18}O$, $\delta^{13}C$, AMS-^{14}C Ages	
0006*	69°12'N	16°49'W	950	3.33	1, 11,	5
0020*	67°59'N	18°32'W	858	23.33	1, 11,	5
16343	66°56'N	07°28'E	1043	26.16	1	
16396	61°52'N	11°15'W	1145	16.05	1	
17045*	52°26'N	16°39'W	3663	6.55	1, 12,	3
17048	54°18'N	18 10'W	1859	11.54?	1, 12	
17049	55°16'N	26°44'W	3331	11.63	1	
17701	68°30'N	10°51'E	1421	8.37	1	
17719	72°09'N	12°35'E	1823	26.74	1	
17724	76°00'N	08°20'E	2354	2.91	1	
17725	77°28'N	04°35'E	2580	?	1	
17728	76°31'N	03°57'E	2485	?	1	
17730*	72°03'N	07°19'E	2769	4.07	1	3

Table 1. (continued)

Core	Latitude	Longitude	Water Depth, m	Sedimentation Rate Across Termi-nation I, cm/kyr	DataSource/ Laboratory for $\delta^{18}O$, $\delta^{13}C$, AMS-^{14}CAges	
17732	71°37'N	04°13'E	3103	8.14	1	
21291	78°00'N	08°03'E	2400	?	1	
21295*	78°00'N	02°25'W	3112	1.76	8	8
21535*	78°45'N	01°51'E	2557	?	1, 14	5
21736	74°20'N	05°10'W	3460	?	1	
21842*	69°27'N	16°31'W	982	3.33	2	6
21900	74°32'N	02°20'W	3538	?	1	
21906	76°30'N	02°05'W	2939	2.91	1	
21910	75°37'N	01°20'E	2454	3.53	1	
23039	67°39'N	05°48'E	1428	?	1	
23040	67°00'N	07°47'E	967	?	1	
23041	68°41'N	00°14'E	2258	2.33	1	
23043	70°16'N	03°21'W	2133	2.33	1	
23055	68°25'N	04°01'E	2311	2.44	1	
23059	70°18'N	03°07'W	2283	1.74	1	
23062	68°44'N	00°10'E	2244	2.33	1	
23063	68°45'N	00°00'E	2299	2.33	1	
23064	68°40'N	00°19'E	2571	2.56	1	
23065	68°30'N	00°49'E	2804	2.21	1	
23068	67°50'N	01°30'E	2230	4.19	1	
23071*	67°05'N	02°55'E	1308	6.84	1	3
23074	66°40'N	04°55'E	1157	20.35	1	
23199	68°23'N	05°14'E	1968	5.29	1	
23205	67°37'N	05°46'E	1411	?	1	
23243	69°23'N	06°33'W	2715	3.53	1	
23246	69°24'N	12°52'W	1858	1.39	1	
23254	73°07'N	09°38'E	2273	7.56	1	
23256	73°11'N	10°57'E	2061	6.40	1	
23258	75°00'N	13°58'E	1768	56.98	1	
23259*	72°02'N	09°16'E	2518	9.30	1	3
23260	72°08'N	11°27'E	2089	8.14	1	
23261	72°11'N	13°06'E	1628	20.58	1	
23262	72°14'N	14°26'E	1130	116.15	1	
23269	71°27'N	00°40'E	2872	?	1	
23294	72°22'N	10°36'W	2224	2.24	1	
23323	67°46'N	05°56'E	1286	?	1	
23331	66°52'N	07°50'E	834	?	1	
23353	70°34'N	12°44'W	1394	7.05	1	
23359	65°32'N	04°09'W	2822	?	1	
B 78-2/2	64°59'N	09°14'E	165	16.67	1	
BOFS 5K*	50°41'N	21°52'W	3547	4.65	4	3
BOFS 8K	52°30'N	22°04'W	4045	16.09	4	
BOFS 11K	55°12'N	20°21'W	2004	2.24	4	
BOFS 14K	58°37'N	19°26'W	1756	1.98	4	
BOFS 17K	58°00'N	16°30'W	1150	3.05	4	
CH 72-101	47°38'N	08°29'W	1925	?	3	
CH 73-110	59°30'N	08°56'W	1365	14.14?	3	
CH 73-136	55°34'N	14°28'W		?	3	
CH 73-139*	54°38'N	16°21'W	2209	10.47	3	3
CH 77-07	66°36'N	10°31'W	1487	7.56	3	
FRAM 1/4	84°30'N	08°59'W	3820	1.54	16	
FRAM I/7	83°53'N	06°57'W	2990	1.40	16	
HM 100-7	61°40'N	04°43'W		?	2	
HM 52-43*	64°15'N	00°44'E	2781	6.03	2	3
HM 71-12	68°26'N	13°52'W	1547	3.26	2	
HM 71-14	69°50'N	18°05'W	1624	3.72	2	
HM 71-15	69°59'N	17°26'W	1547	?	2	
HM 71-17	70°00'N	13°01'W	1460	?	2	
HM 71-19	69°29'N	09°31'W	2210	2.56	2	
HM 79-4/6*	63°06'N	02°33'E	900	38.00	2	3
HM 79-26	66°54'N	05°56'W	3312	2.14	2	
HM 80-30	71°47'N	01°36'E	2821	2.09	2	
HM 80-42	72°15'N	09°14'W	2416	3.45	2	
HM 80-60	68°54'N	11°51'W	1869	12.03?	2	
HM 94-13*	71°38'N	01°38'W	1946	2.59	2	6

Table 1. (continued)

Core	Latitude	Longitude	Water Depth, m	Sedimentation Rate Across Termi-nation I, cm/kyr	DataSource/ Laboratory for $\delta^{18}O$, $\delta^{13}C$, AMS-^{14}CAges	
HM 94-18	74°30'N	05°41'E	2469	2.79	2	
HM 94-25*	75°36'N	01°18'E	2469	1.84	2	6
HM 94-34*	73°46'N	02°32'W	3004	1.37	2	6
K 11	71°47'N	01°36'E	2900	2.91	3	
KN 708-1	50°00'N	23°45'W	4053	?	7	
KN 714-15	58°46'N	25°47'W	2598	?	7	
MG 123	79°16'N	00°48'E	3050	6.16	1	
NA 87-22*	55°30'N	14°35W	2161	?	3	
ODP 609*	50°00'N	24°00'W	3900	?	13	13
SO 82/5	59°11'N	30°54'W	1416	?	1	
SU 90-32	61°47'N	22°25'W	2200	?	3	
SU 90-39	53°00'N	22°00'W	?	?	3	
SU 90 I07	63°05'N	28°05'W	1625	4.11	3	
SU 90 I08	60°35'N	22°05'W	2395	2.47	3	
TROLL 3.1*	60°47'N	03°43'E	332	212.67	10	
UB 25-09	63°03'N	04°47'E	600	33.11	1	
UB 28-18	62°56'N	02°44'E	770	43.62	2	
UB 31-33	63°38'N	01°46'E	1580	16.75	1	
UB 31-36	64°15'N	00°31'E	2620	?	1	
V 23-42	62°11'N	27°56'W	1514	?	8	
V 23-81*	54°02'N	16°08'W	2393	12.71	2	
V 23-83	49°52'N	24°15'W	3971	?	8	
V 27-86	66°36'N	01°07'W	2900	?	3	
V 27-114	55°03'N	33°04'W	2532	?	8	
V 27-116	52°50'N	30°20'W	3202	?	8	
V 28-14*	64°47'N	29°34'W	1855	6.94	9	15
V 28-38	69°23'N	04°24'W	3411	8.37	3	
V 28-56	68°02'N	06°07'W	2941	4.65	3	
V 29-183	49°08'N	25°30'W	3629	?	8	
V 29-206	64°54'N	29°17'W	1624	?	8	
V 30-108	56°06'N	32°30'W	3171	?	8	

Notations are 1 University of Kiel; 2 University of Bergen; 3 Centre des Faibles Radioactivités, Laboratoire mixte CNRS-CEA, Gif sur Yvette; 4 Godwin Laboratory, Cambridge; 5 ETH Zürich; 6 Uppsala; 7 Ruddiman and McIntyre [1981]; 8 Keigwin and Boyle [1989]; 9 Curry et al. [1988]; 10 Lehman et al. [1991], 11=Lackschewitz [1991], 12 K. Winn, unpublished data, 1991; 13 Bond et al. [1993], 14=Köhler [1991], 15=Bard et al. [1994], 16 Zahn et al. [1985].

* AMS-^{14}C dated cores.

paleodensity distribution of surface water and to identify sites of potential paleodeepwater formation [*Labeyrie et al.*, 1992]. Finally, the reconstructed paleocurrent patterns can be compared with patterns deduced from ice-rafted debris (IRD). *Bischof* [1990] and *Henrich* [1992] traced ice-rafted coal particles in sediment cores back to Svalbard and the North Norwegian shelf and Cretaceous *Inoceramus* debris back to the North Sea. They concluded that, like today, an anticlockwise circulation largely persisted in the Nordic Seas over glacial and interglacial times, except for short phases with a particularly puzzling distribution pattern off Norway, such as during early glacial Termination I [*Bischof*, 1990].

It is a special objective of our study to trace the sources and refine the dispersion patterns of past meltwater events in the Nordic Seas and northeastern North Atlantic, previously described in this region by *Jones and Keigwin* [1988], *Lehman et al.* [1991], *Veum et al.* [1992], *Weinelt et al.* [1991], *Lehman and Keigwin* [1992], and *Sarnthein et al.* [1992]. Most of these events were probably linked to rapid atmospheric changes as reflected by Dansgaard-Oeschger events in Greenland ice cores [*Dansgaard et al.*, 1993; *Bond et al.*, 1992, 1993]. *MacAyeal* [1993] proposed that the meltwater events were induced by "binge/purge" oscillations of the main ice sheets in the northern hemisphere, which produced surges and flotillas of melting icebergs during phases of both glacial melt and glacial advance. Such a mechanism, however, still requires detailed tests. Our study tries to search for high-resolution records that reflect the possible leads and lags or synchronism of major meltwater pulses found in front of the various LGM ice sheets near to the western and eastern North Atlantic to locate more precisely the sites of initial meltwater/climatic forcing. Prevalent point sources of meltwater generation may enable us to distinguish the isotopic signal of meltwater from that of the general background of sea surface water.

Methods and Strategies

This study is based on $\delta^{18}O$ values of *N. pachyderma* (s) (125-250 μm) that are generally considered as a signal of the temperature-salinity regime in the upper 50 m of surface water. The exception to this is near oceanic fronts and near sea ice margins, such as in the modern Fram Straits, where warm and nutrient-rich surface water submerges below polar water and *N. pachyderma* (s) concentrates in the deepening thermocline [*Carstens and Wefer*, 1992]. Likewise, $\delta^{13}C$ records of *N. pachyderma* are used as a tracer of the nutrient concentrations and thus of the ventilation state of the surface water [*Johannessen et al.*, 1994]. Moreover, we expect that

strong convection and enhanced gas exchange between the atmosphere and the ocean are documented by high $\delta^{13}C$ values such as in the modern Arctic domain of the Greenland and Iceland Seas [*Koltermann*, 1987; *Johannessen et al.*, 1994].

The isotope measurements (Figure 3 and figures in electronic supplement[1]) were mainly performed by the Bergen and Kiel laboratories. Some additional data were taken from the literature (Table 1). Both laboratories use Finnigan MAT 251 mass spectrometers. The Kiel laboratory uses a Carbo-Kiel preparation line which is an automated system in which acid is added to individual samples, reacted at 90°C. The analytical reproducibility based upon replicate measurements of an internal laboratory standard is ±0.04 for $\delta^{13}C$ and ±0.07 for $\delta^{18}O$. The Bergen laboratory uses an automated version of the manual system described by *Shackleton et al.* [1983] in which acid is dropped into individual sample chambers and the sample is reacted at 50°C. The analytical reproducibility is ±0.06 for $\delta^{13}C$ and ±0.07 for $\delta^{18}O$. Both laboratories calibrate to the peedee belemnite (PDB) scale via the National Bureau of Standards (NBS) 19 standard.

As a check of the intercalibration of the two laboratories, the Bergen laboratory standard, which is a Leonardo (LEO) Carrara marble powder, was analyzed in Kiel. The Bergen values for this standard are 2.04 for $\delta^{13}C$ and -1.88 for $\delta^{18}O$. The Kiel measurements gave the values 2.04 ±0.02 for $\delta^{13}C$ and -1.86±0.08 for $\delta^{18}O$ (seven measurements). The excellent agreement of these results documents that data from the two labs can be readily interchanged, with no substantial introduction of errors. This also appears to be the case for samples of higher $\delta^{18}O$ values. In all time slices we observe that the patterns do not depend on the laboratory which performed the measurements. For example, when adding data from one lab to a cluster of data points from another lab a new value does not change the already existing patterns.

Paleotemperature (SST) estimates (Figure 4) employed for interpreting the $\delta^{18}O$ records of various time slices, are based on species counts of planktonic foraminifera [*Schulz*, 1994] and the "maximum similarity" (SIMMAX-26) transfer function technique [*Pflaumann and Hensch*, 1994] that improves on the SIMMAX-24 equation of *Pflaumann et al.* [1995]. The standard deviation of the residuals of this equation is ±1.03°C for summer SST of 3-28°C. With SSTs decreasing from 3.5° to -2°C the error gradually shifts to a range of 0 to +3.5° (i.e, at -1.7°C the estimates deviate between -1.7° and 1.5°C), probably a result of the decreasing seasonal time span permitting foraminiferal growth.

The reconstruction of any paleowater mass is based on several data points each in the time-slice maps and on a careful interpolation between the individual data points using (visual) triangulation, a technique that turned out to be superior to both kriging and splining techniques [*Schäfer-Neth*, 1994]. Prior to plotting, the data sets were culled in two steps. A great number of poor isotopic records were simply omitted ("n.i." in table available on electronic supplement; see footnote 1). Moreover, data from records that lack an appropriate sampling resolution and/or clear $\delta^{18}O$ stratigraphy or the sedimentation rates of which may be too low to resolve the full amplitude of any particular isotopic event are marked in the electronic supplement table and the time-slice figures. Finally, the consistency of the inferred paleoceanographic patterns was supported by the finding that adding any additional core records finally induced little change in the course of the isolines (e.g, core HM 1007 near Faeroe in the maps of the last glacial maximum and other time slices).

Patterns of paleodensity (σ_{ST}) were estimated from both the planktonic $\delta^{18}O$ values and SST data, following the graphical approach of *Cox et al.* [1970], *Duplessy et al.* [1991], and *Labeyrie et al.* [1992]. At summer SST near 3°-6°C the error of density estimates lies at about ±0.35 σ_{ST}, a range mostly sufficient to sort out potential areas of paleodeepwater convection. At summer SST of less than 3°C, the error gradually shifts to +0.6/-0.0 σ_{ST}.

Paleocurrent tracks were derived from the assumption that geostrophic circulation dominates over wind-driven circulation in latitudes higher than 50°N. Thus a surface-water mass with a density maximum in its center (marked by both high $\delta^{18}O$ and lower SST values) is turning anticlockwise/ cyclonic, and vice versa, a water mass with a low-density core (with low $\delta^{18}O$ values and low to medium high SST in the center, as characteristic of meltwater lenses) is turning clockwise because of geostrophic considerations.

(The data sets ("Norwegian-Greenland Sea (NGS) time slices" and *Schulz* [1994]) are available on request from the German "Past Global Changes" (PAGES) marine data repository SEPAN (grobe @ awi-bremerhaven.de).)

Age Control

Our time-slice reconstructions are based on stratigraphic correlations using well-defined stratigraphic events (Table 2) in 110 $\delta^{18}O$ curves of *N. pachyderma* (sin), which were AMS-^{14}C dated in 21 sediment cores back to about 35 ka (Table 1; Figure 3; locations in Figure 2). The $\delta^{13}C$-corrected ^{14}C years B.P. were reduced for the ocean-reservoir effect of 400 years (Table 3 shows new unpublished AMS-^{14}C ages, measured in Gif-sur-Yvette and Uppsala). Many of the radiocarbon dated cores have high sedimentation rates exceeding 5-10 cm/kyr, and hence allow the clear definition of the ages of $\delta^{18}O$ events. Foraminiferal dissolution is of minor importance in cores from the Nordic Seas, except for short intervals at deglaciations [*Henrich*, 1992]. We do not believe that dissolution affects the isotopic record to any significant degree because (1) most core locations are relatively shallow, and (2) the isotopic patterns remain robust in cores with differing dissolution.

Apart from a few core locations on the upper margins (at less than 1000-m water depth) foraminiferal concentrations do not vary systematically in the Norwegian Sea from interglacial to glacial times, except for minima during Termination I (Figure 4). Smearing by bioturbation is not likely to create artificially the extreme $\delta^{18}O$ minima that are picked in some time slices because (1) they tend to coincide with minima in foraminifera abundance and hence would most likely be smoothed by mixing from high to low abundance, and (2) low foraminifera abundances are not linked to dissolution but rather to dilution by short lasting extreme

[1]An electronic supplement of this material may be obtained on a diskette or Anonymous FTP from KOSMOS.AGU.ORG. (LOGIN to AGU's FTP account using ANONYMOUS as the username and GUEST as the password. Go to the right directory by typing CD APEND. Type LS to see what files are available. Type GET and the name of the file to get it. Finally, type EXIT to leave the system.) (Paper 95PA01453, Variations in Atlantic surface ocean paleoceanography, 50°-80°N: A time-slice record of the last 30,000 years, M. Sarnthein et al.). Diskette may be ordered from American Geophysical Union, 2000 Florida Avenue, N.W., Washington, DC 20009; $15.00. Payment must accompany order.

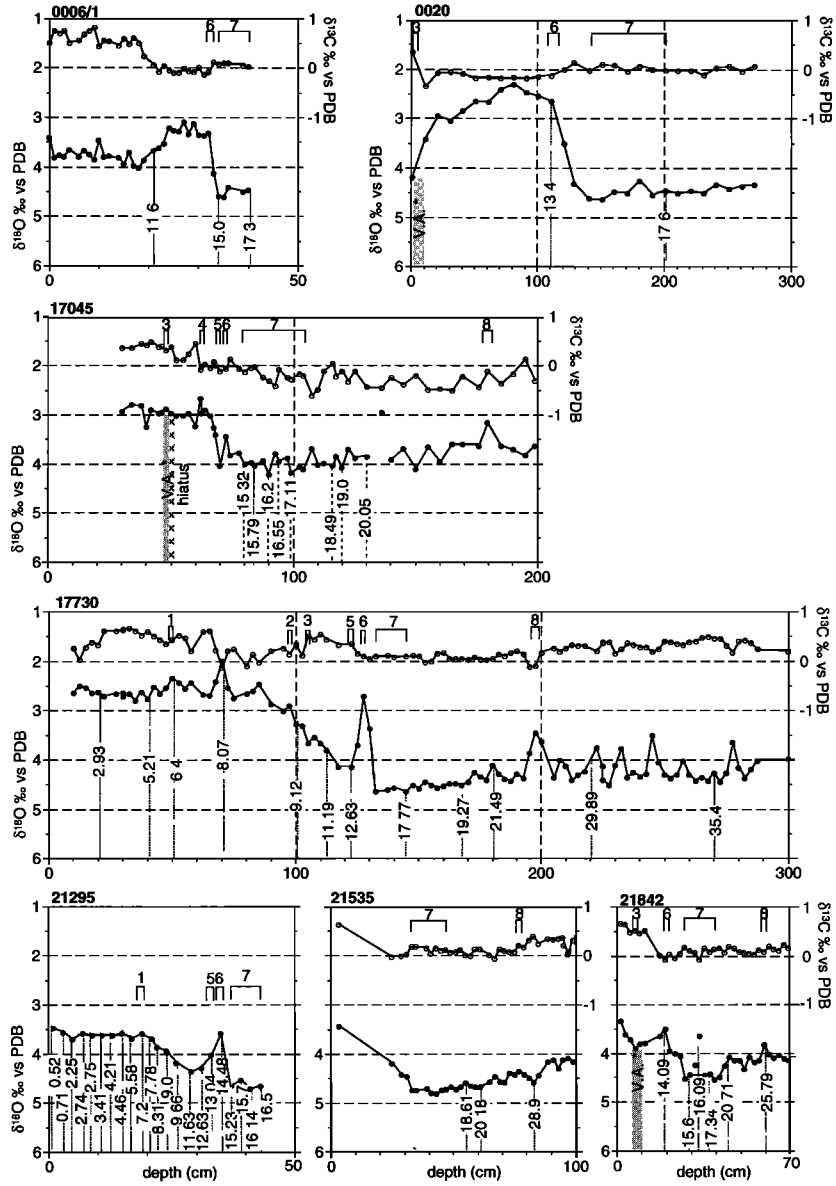

Figure 3. AMS-^{14}C dated (numbers in ka) $\delta^{18}O/\delta^{13}C$ records of *Neogloboquadrina pachyderma* (s) from the North Atlantic 50°-80°N. Horizontal bars mark time slices 1-8: 1, 6.5 ^{14}C ka; 2, 9.0 ^{14}C ka; 3, Younger Dryas; 4, 10.8 - 10.3 ^{14}C ka; 5, 12.8-12.6 ^{14}C ka; 6, 14.2-13.2 ^{14}C ka; 7, LGM; 8, 26.0 ^{14}C ka). Zigzag line in core 17045 marks hiatus. V.A. is the Vedde ash. Sources of $\delta^{18}O/\delta^{13}C$ records and AMS ^{14}C ages are in Table 1.

siliciclastic sedimentation rates that reduce the impact of bioturbational mixing.

Linear age interpolations (assuming constant sedimentation rates between age control points) were calculated in the domain of "adjusted" calendar years only (the term "adjusted" was proposed by N.J. Shackleton to the European paleoclimatic working group for ^{14}C dates converted into calendar years). This conversion of ^{14}C ages into calendar years is following *Winn et al.* [1991] and is necessary because the relationship between the two timescales is telescopic and, in part, *nonlinear* because of major "^{14}C plateaus" near 10,200-9,600 and 12,750-12,500 ^{14}C years B.P., as demonstrated by (1) the U/Th datings of *Bard et al.* [1990], (2) the dendrochronology of *Becker and Kromer* [1993], (3) the ice varve stratigraphy of *Taylor et al.* [1993], and (4) the sediment varve stratigraphy of *Lotter et al.* [1992]. Thus any direct use of radiocarbon years necessarily produces biased estimates of interpolated sediment ages and sedimentation rates. We applied the dendrochronological ages of *Kromer and Becker* [1993] for converting the radiocarbon ages of the last 10,000 years and the U/Th datings of *Bard et al.* [1990] for converting the ^{14}C ages of glacial Termination I and oxygen isotope stage 2 into calendar years. For convenience, the interpolated calendar years were finally reconverted into ^{14}C years so that they are comparable to other studies where ages are given in ^{14}C years B.P.

Eight time slices were defined and age interpolated by means of the following features in the $\delta^{18}O$ record and also

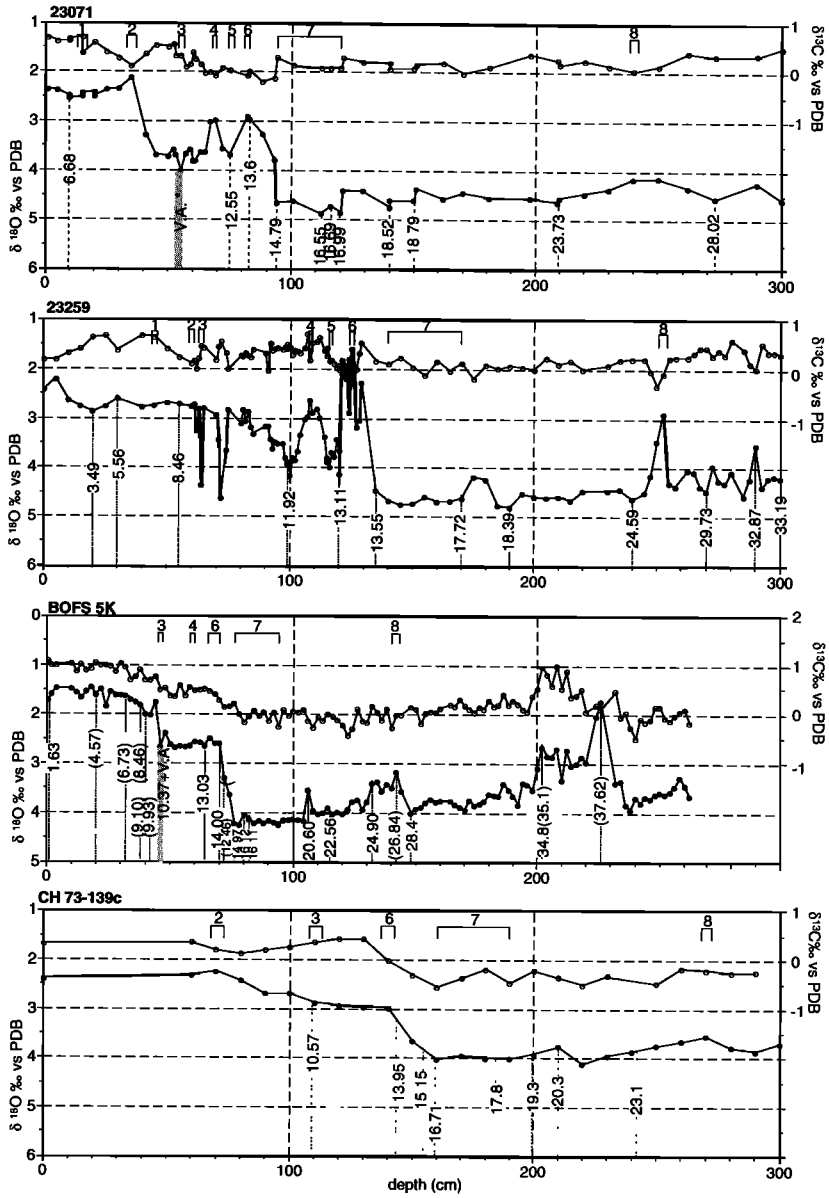

Figure 3. (continued)

from correlated $\delta^{13}C$ records (age intervals of time slices marked as bars on $\delta^{18}O$ records in Figures 3 and 4; $\delta^{18}O/\delta^{13}C$ values given in electronic supplement table):

Time slice 8, "26,000 ^{14}C years B.P." ($\delta^{18}O$ event 3.1), equal to 29,500 cal years B.P., picks (mostly) single values from a short lasting $\delta^{18}O$ minimum near the end of stage 3, which was dated by AMS ^{14}C ages to 25,5-26,9 ka (Figure 3). At cores that lack the short minimum we selected the upper end of a $\delta^{18}O$ "shoulder" at the end of stage 3, prior to the $\delta^{18}O$ increase by >0.5 ‰ into cold stage 2. The search for the end of stage 3 was facilitated by the first occurrence *Siphotextularia rolshauseni,* a benthic foraminifera that is common in the subsequent stage 2 [*Struck and Nees*, 1991].

Time slice 7, "last glacial maximum," employs average values of all data in the $\delta^{18}O$ maximum range, connected by a line in Figure 3 and the electronic supplement figure between 17,700 and 15,000 ^{14}C years B.P., equal to 21,200-18,500 cal years B.P. This time slice ends at the inflection point in the $\delta^{18}O$ curves, which marks the first strong $\delta^{18}O$ reduction, defined as the onset of Termination IA [*Duplessy et al.*, 1981]. In cores from the northeast Atlantic the top portion of the LGM style $\delta^{18}O$ records of *N. pachyderma* has been ignored, if $\delta^{18}O$ records of other, especially benthic, foraminifera species indicate the onset of Termination IA farther downcore (not depicted).

Time slice 6,"14,200-13,200 ^{14}C years B.P.," was selected because of an extreme $\delta^{18}O$ minimum at the beginning of Termination IA, best defined in Norwegian Sea cores 17730, 23071, and 23259 (Figures 1 and 3) where average sedimentation rates exceed 7-10 cm/kyr. The ^{14}C age corresponds to about 17.7-16.7 cal ka, perhaps to 17.7-16.2 cal ka (i.e., 1500 years), because the precise range of ^{14}C plateaus is yet unknown in this interval. A slightly higher ^{14}C age (14.48 ka) of the $\delta^{18}O$ minimum in core PS 21295 [*Jones and Keigwin*,

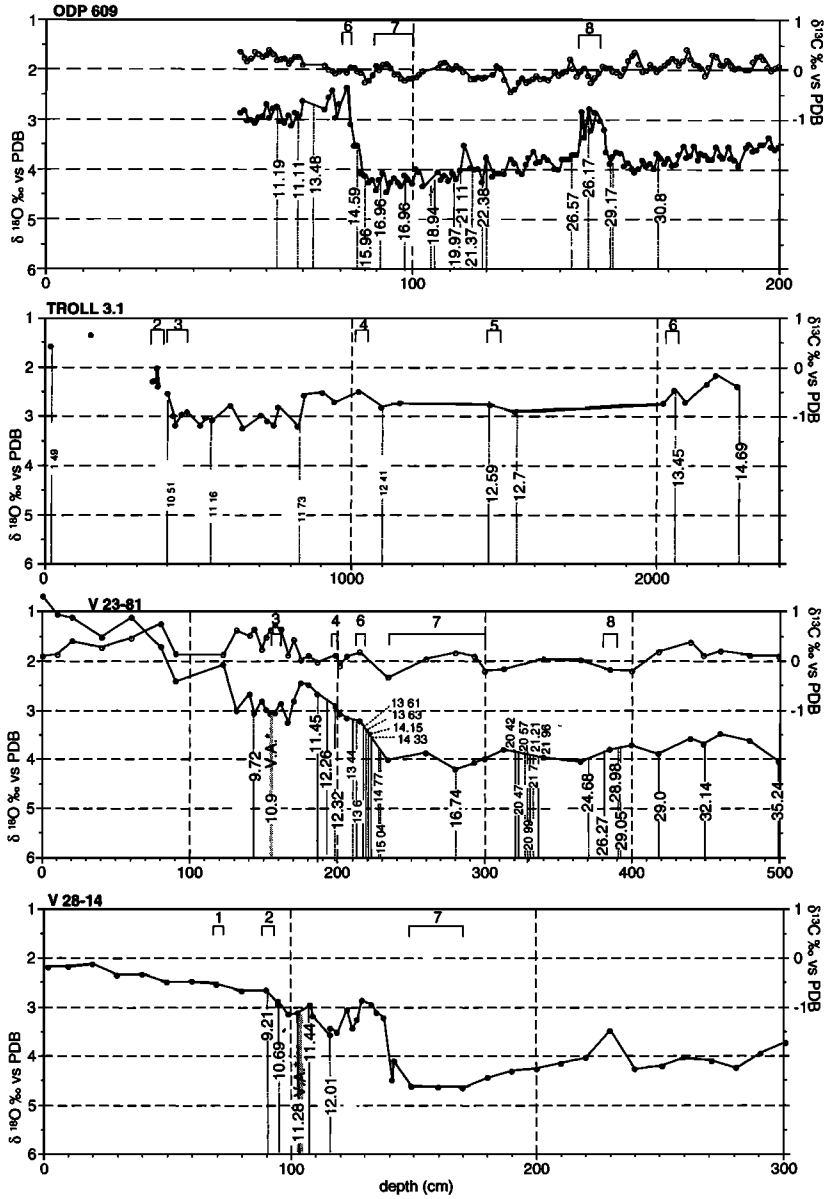

Figure 3. (continued)

1989] appears to be linked to bioturbational mixing at very low sedimentation rates of <2 cm/kyr. The majority of ^{14}C ages in high-sedimentation rate cores converge to 14.2-13.2 ka, paralleling the Oldest Dryas cold spell. Hence this $\delta^{18}O$ minimum, which represents the first great meltwater event in the Nordic Seas subsequent to the LGM [*Jones and Keigwin*, 1989] may be a few hundred years younger than Heinrich layer 1 in the North Atlantic [*Bond et al.*, 1992]. In cores with high sedimentation rates (>10-20 cm/kyr), time slice 6 picks the lowest $\delta^{18}O$ value out of a number of negative $\delta^{18}O$ excursions. In these spikes, the maximum variations of microfossil concentration (Figure 3) parallel highest signal amplitudes. Hence bioturbational smearing is not likely to matter because these records would be most strongly affected by mixing from high to low intervals. In cores from the southern Norwegian Sea and outside, the event is reduced to a distinct shoulder in the $\delta^{18}O$ decrease of Termination IA (TROLL 3.1, UB 25-9, BOFS 5K, CH 73-139, V23-81; Figure 3).

Time slice 5, "12,800-12,600 ^{14}C yr B.P." (equal to >>14,800-14,600 cal years B.P.), selects a short, but consistent, $\delta^{18}O$ maximum in the Nordic Seas after the first, meltwater related $\delta^{18}O$ minimum of Termination IA (best dated in cores 17730, 23071, 23259, HM 79-6/4, and TROLL 3.1). In reality, time slice 5 probably covers a longer time span (700 years ?) than indicated by ^{14}C age, because it matches a major ^{14}C plateau marking this phase of deglaciation and the turn-on of North Atlantic Deep Water formation [*Sarnthein et al.*, 1994].

Time slice 4, 12,400-12,100 ^{14}C years B.P." (equal to 14,400-14,100 cal years B.P.), picks a second major $\delta^{18}O$ minimum and meltwater event in the Norwegian Sea. Generally, it is separated from the preceding $\delta^{18}O$ minimum by the $\delta^{18}O$ maximum of time slice 5. The age is best constrained in high-

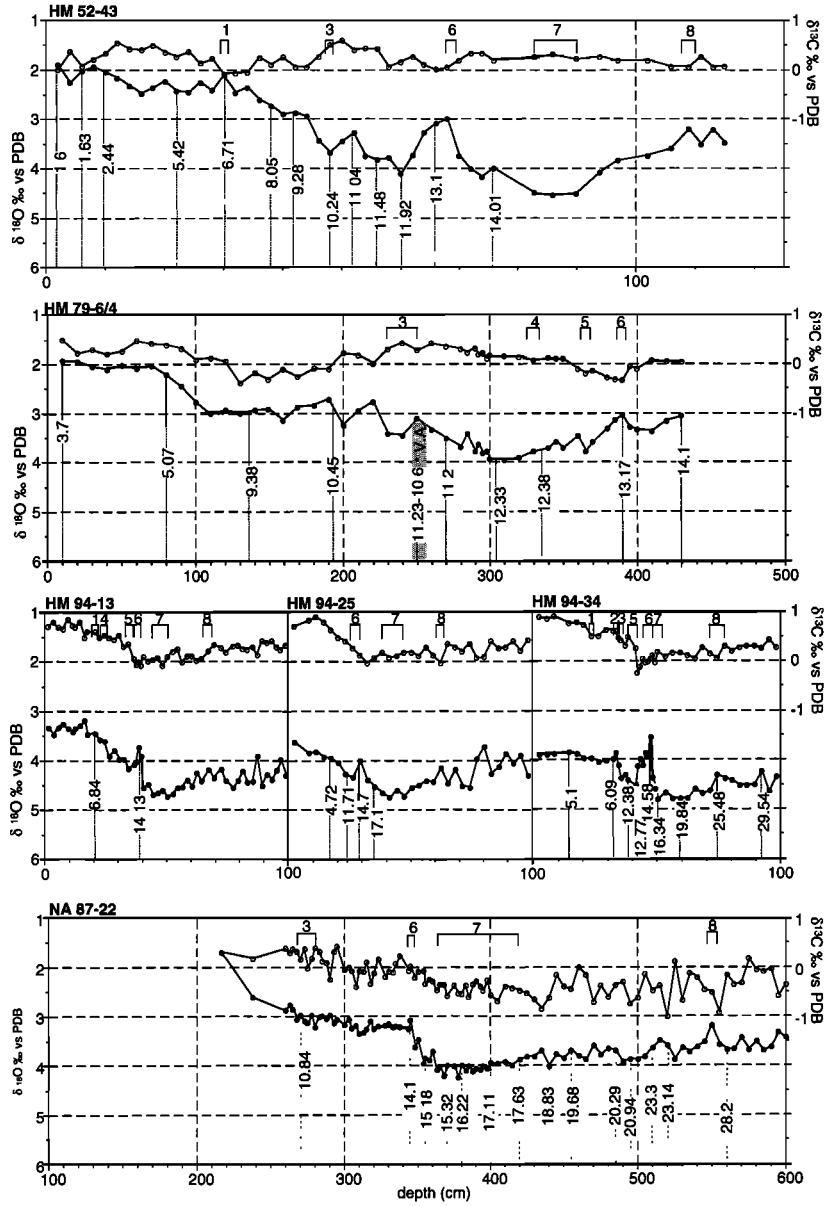

Figure 3. (continued)

sedimentation rate cores 23071 and 23259 (Figure 3) and corresponds to the late Bölling warm phase.

Time slice 3, 10,900-10,300 ^{14}C years B.P." (equal to 12,900 - <<12,300 cal years/ -?11,700 cal years B.P.), employs the $\delta^{18}O$ average values of the Younger Dryas. It ends with an inflection point in the $\delta^{18}O$ record and, more clearly, with a minimum or inflection point in the SST curve (Figures 3 and 4, electronic supplement figure), points that mark the onset of Termination IB. In many cores from the southern Nordic Seas and the northeastern North Atlantic, the identification of the Younger Dryas was facilitated by the Vedde ash layer [*Mangerud et al.*, 1984] with an average ^{14}C age of 10.6 ka (possibly 10.3 ka) (E. Bard, personal oral communication, 1993). In many cores from the northeast Atlantic it turned out to be difficult to define the Younger Dryas cold spell in the $\delta^{18}O$ records because *N. pachyderma* (s) disappears almost completely in lower Holocene sediments [*Schulz*, 1994]. Thus *pachyderma* (s) tests with a "cold" isotopic signal were strongly bioturbated upcore, by up to >25 cm into sediments above the Vedde ash layer.

Time slice 2, 9,200-9,000 ^{14}C years B.P." (equal to about 9900-9600 cal years B.P.), picks a single value from the well defined first $\delta^{18}O$ minimum spike or shoulder at/or slightly below the onset of the Holocene $\delta^{18}O$ plateau. The event represents both a major warming of SST and the last, mostly minor meltwater influence felt in the marginal Norwegian Greenland Sea. The time slice is directly dated and/or closely interpolated in AMS-^{14}C dated cores, where (1) the Holocene is preserved, and (2) *N. pachyderma* (s) is common in the Holocene. In some cores from the northeast Atlantic upcore biotur-

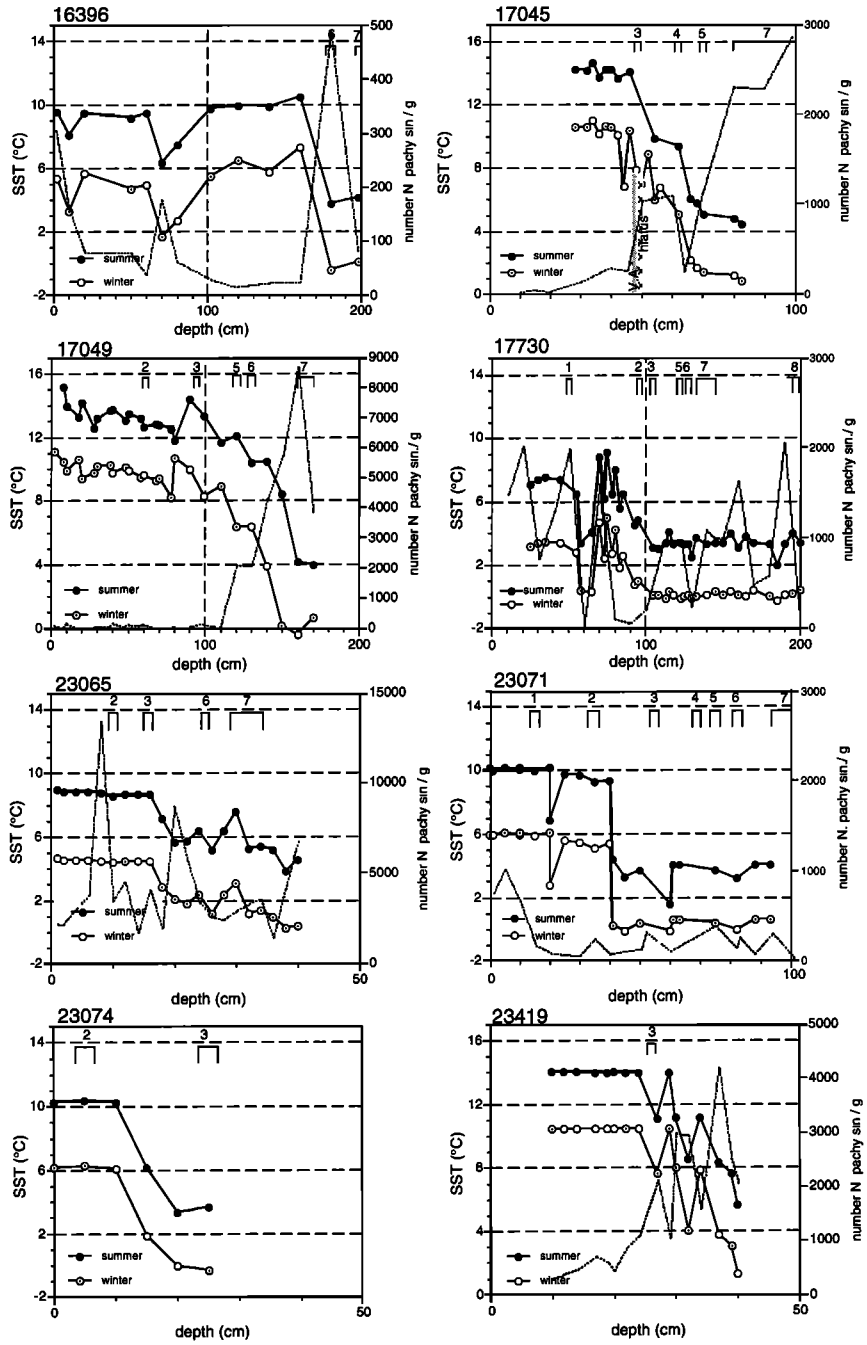

Figure 4. Sea surface temperature (SST) records in deep-sea cores from the North Atlantic 50°-80°N. Horizontal bars mark time slices 1-8 (see electronic supplement table). Dotted lines show abundance concentrations of *N. pachyderma* (s).

bation has shifted the antecedent cold $\delta^{18}O$ signal of *N. pachyderma* (s) into the Holocene section ("n.i." for time slice 2 in electronic supplement table).

Time slice 1, 7000-6000 ^{14}C years B.P." (equal to about 7900/7815-6850 cal years B.P.), represents the peak Holocene climate, when SSTs reached a maximum at several sites (Figure 4), some $\delta^{18}O$ records showed a further slight decrease, and meltwater fluxes were virtually absent in the Nordic Seas. Time slice 1 picks single or average $\delta^{18}O$ values by means of linear age interpolation between 9.8 cal ka at the $\delta^{18}O$ "shoulder" of the early Holocene and the sediment surface of cores in which the age of the core top was unequivocally identified as "modern." In gravity and kasten cores without AMS ^{14}C dates, the actual sediment surface was obtained by splicing the topmost $\delta^{18}O/\delta^{13}C$ records with records of neighboring box cores where both the true sediment surface and the top of Termination I are clearly identified [*Vogelsang*, 1990].

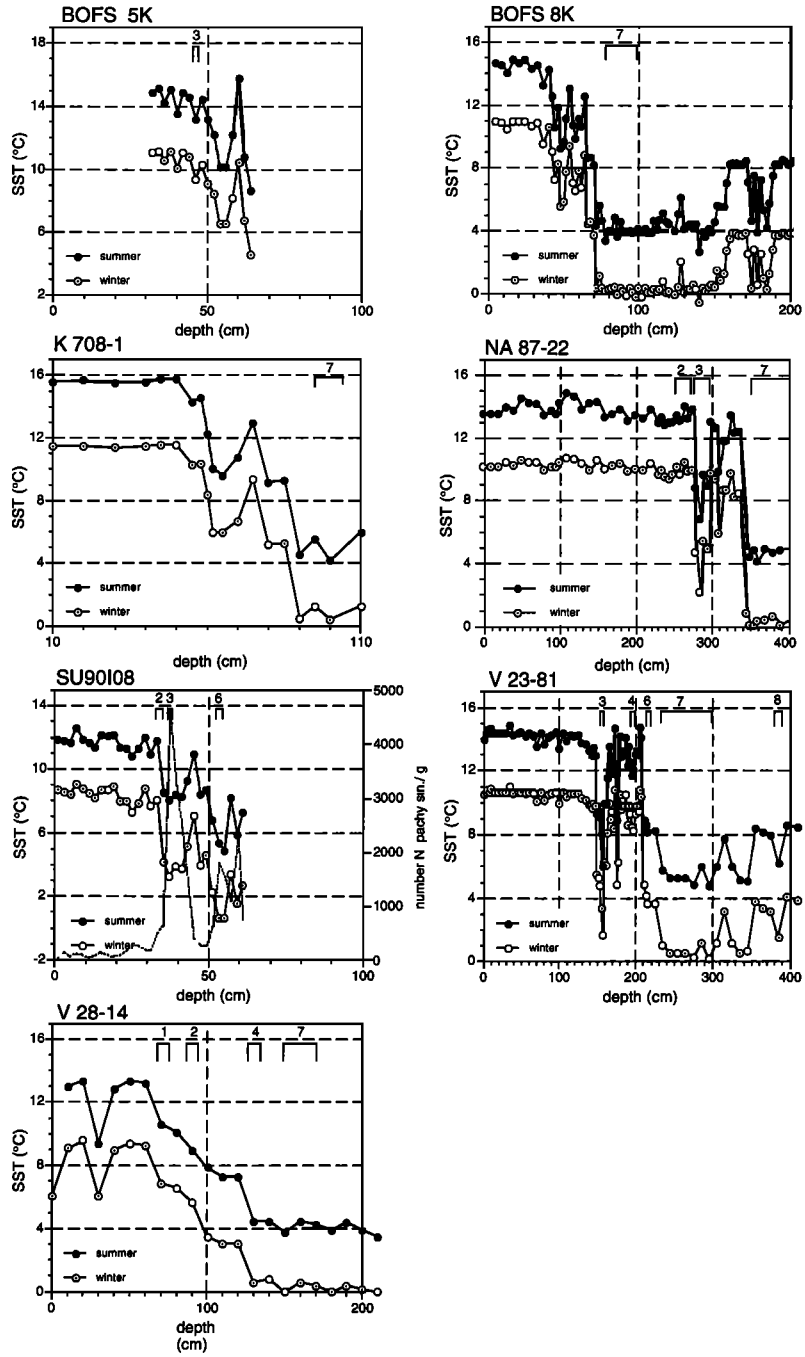

Figure 4. (continued)

Modern Distribution Patterns of Planktonic $\delta^{18}O$ and $\delta^{13}C$

The modern distribution of core top isotope data for *N. pachyderma* (s) in the study area (Figure 5) was compiled from cores with good Holocene resolution and a well-preserved sediment surface. In many cases, the core top samples were taken from box cores containing a well-preserved sediment surface from the immediate neighborhood of a gravity or kasten core, in which the sediment surface usually is damaged. The core fits between the neighboring box and gravity/ kasten cores were reconstructed from the match of isotopic curves. The number of modern data points are less for $\delta^{13}C$ than for $\delta^{18}O$ because some published data sets only give $\delta^{18}O$.

The isotopic distributions are a clear reflection of the salinity/temperature fields (x/y graph from *Weinelt et al.* [1996]) and the circulation regime of the present Nordic Seas, hence giving credit to the use of isotopic distributions to infer past surface ocean circulation patterns. Along the eastern continental margin, a strong meridional signal is evident in the $\delta^{18}O$

Table 2. Age Definition of $\delta^{18}O$ Stratigraphic Events

Age, ^{14}C kyr B.P.	$\delta^{18}O$ Record	Event
9,000	beginning of $\delta^{18}O$ plateau	begin Holocene/ end of Termination IB
10,300	$\delta^{18}O$ maximum/ end of plateau	approximate end of Younger Dryas on top of Vedde ash layer
12,400-12,100	$\delta^{18}O$ minimum	Second meltwater event in Termination I
12,800-12,600	$\delta^{18}O$ maximum	
14,200-13,200	$\delta^{18}O$ minimum	first meltwater event in Termination IA, corresponding to Heinrich event 1?
17,700-15,000	$\delta^{18}O$ maximum	last glacial maximum
26,000	$\delta^{18}O$ minimum	Isotope stage 3.1/ Heinrich event 3

data, documenting a progressive cooling of warm waters flowing from the northeast Atlantic ($\delta^{18}O$ <1‰) into the southeastern Norwegian Sea (<2‰) and extending in a narrowing corridor all the way past Svalbard (2.7-2.9‰). This corridor of warm waters is clearly separated from the heavier $\delta^{18}O$ of the cold regions in the west, and the Arctic Front is easily seen in the distribution pattern (>3‰ isoline). The heaviest values belong to the central gyres in the Greenland and Iceland Seas and the East Iceland Current. In the far east, the lower salinities of the Norwegian Coastal Current are recorded by lower $\delta^{18}O$ values, and in the far west (core HM 71-14; see electronic supplement figure), $\delta^{18}O$ values drop in connection with the lower salinities of the polar waters of the East Greenland Current. Farther south, the Irminger Current is documented by low $\delta^{18}O$ values west of Iceland (cores SU 90 I07 and V 28-14; Figure 3 and electronic supplement figure).

The two gyres in the Iceland and Greenland Seas are even more clearly depicted by the $\delta^{13}C$ distribution, where the gyre centers have the highest values (>0.7‰) and the warmer Atlantic waters flowing northward and in a branch toward Jan Mayen Island carry a lower $\delta^{13}C$ signal of <0.3‰.

Combining the $\delta^{18}O$ and $\delta^{13}C$ patterns, we observe that the convective regions in the present Nordic Seas, i.e., in the Greenland and Iceland Seas, are characterized by combined high values in both carbon and oxygen isotopes. As noted by *Johannessen et al.* [1994], this observation presents a strong clue as to how convective regions can be defined in the past.

The perennially sea-ice-covered central Arctic Ocean displays isotopic values of *N. pachyderma* that range near 1.4-2.2‰ $\delta^{18}O$ and 0.8-1.1‰ $\delta^{13}C$ [*Spielhagen and Erlenkeuser*, 1994] and thus are completely different from those in the Nordic Seas.

Past Time Slices

Meltwater Event at Isotopic Event 3.1

Description. The $\delta^{18}O$ distribution patterns at 26 ka indicate E-W gradients and N-S running isolines north of 68°N (Figure 6). A central feature is a tongue-shaped $\delta^{18}O$ minimum (3.75-2.9‰) northwest of the Lofoten Archipelago/northern Norway, which is documented as a "mound" in six high-resolution cores. The heaviest values (4-4.4‰) occur in the central Nordic Seas, confined by somewhat lighter values off East Greenland. The northeast Atlantic sector off Ireland is charac-

Table 3. Unpublished AMS^{14}C Datings, N. pachyderma (s) 1σ errors, and Core Depth of Samples

Depth, cm	^{14}C Age	Reservoir Corrected ^{14}C-Age	Error. 1σ
	>17045<		
80	15,720	15,320	150
84	16,190	15,790	160
90	16,600	16,200	200
94	16,950	16,550	180
99	17,510	17,110	170
116	18,890	18,490	200
120	19,400	19,000	200
130	20,450	20,050	230
	>17730<		
20	3,330	2,930	100
40	5,610	5,210	70
50	6,800	6,400	110
70	8,470	8,070	90
100	9,520	9,120	590
112.5	11,590	11,190	100
122.5	13,030	12,630	120
145	18,170	17,770	160
160	19,670	19,270	220
180	22,890	22,490	330
220	30,260	29,860	590
240	35,800	35,400	1100
270	>45,000		
	>21842<		
18.5	14,490	14090	
28.5	16,000	15600	
32.5	16,490	16090	
36.5	17,740	17340	
44.5	21,110	20710	
60.5	26,190	25790	
	>23071<		
15	7,080	6,680	120
75	12,950	12,550	220
82	14,000	13,600	300
93	15,190	14,790	190
112	16,950	16,550	200
116	17,090	16,690	230
120	17,390	16,990	220

Table 3. (continued)

Depth, cm	^{14}C Age	Reservoir Corrected ^{14}C-Age	Error. 1σ
140	18,920	18,520	240
150	19,190	18,790	240
170	21,830	21,430	300
210	24,130	23,730	360
273	28,420	28,020	560
333	40,000	39,600	1800
	>23259<		
20	3,820	3,420	150
30	5,960	5,560	100
55	8,860	8,460	160
99	12,320	11,920	220
120	13,510	13,110	200
135	13,950	13,550	240
170	18,120	17,720	240
190	18,790	18,390	290
240	24,990	24,590	410
270	30,120	29,720	540
290	33,270	32,870	890
300	33,590	33,190	930
310	40,000	39,600	1700
	>HM 94-13<		
20.5	7,240	6,840	
38.5	14,530	14,130	
	>HM 94-25<		
17.5	5,120	4,720	
23.5	12,110	11,710	
29.5	15,100	14,700	
35.5	17,500	17,100	
	>HM 94-34<		
14.5	5,500	5,100	
32.5	6,490	6,090	
38.5	12,780	12,380	
41.5	13,170	12,770	
47.5	14,980	14,580	
50.5	16,740	16,340	
59.5	20,240	19,840	
74.5	25,880	25,480	
92.5	29,940	29,540	

Data are from the Tandetron Lab, Gif sur Yvette. Ages were obtained at abundance maxima of N. pachyderma (s) to reduce bioturbational bias and corrected for oceanic reservoir effect by -400 years.

terized by a region of heavy values (3.5-3.7‰) surrounded by lighter values. In total, the maximum $\delta^{18}O$ values show a gradient of 0.7‰ between the northeast Atlantic and the Nordic Seas.

The distribution of $\delta^{13}C$ values, which are particularly low in this time slice, shows similarities with the $\delta^{18}O$ results. In general, the lowest values correspond with lighter $\delta^{18}O$ and follow the distinct tendency of lower values along the coasts on both sides of the Nordic Seas (-0.5-0‰ in the east; <0‰ in the SW). The light $\delta^{18}O$ tongue NW of northern Norway is clearly mimicked (with a minor offset) by low $\delta^{13}C$ in five cores. In the northeast Atlantic, west of Ireland, lies the absolute $\delta^{13}C$ minimum of -0.9‰. The maximum $\delta^{13}C$ values (>0.3‰) occur in the central Nordic Seas, somewhat offset from the $\delta^{18}O$ maximum to the north.

Discussion. The $\delta^{18}O$ isotopic distribution pattern, with light values along the margins and isotopically heavy centers, suggests a meridional type of circulation linked to counterclockwise circulation within the Nordic Seas. This is most clearly seen in the northern Norwegian and Greenland Seas where a branch of isotopically light water extends out as a tongue from the Lofoten Archipelago off northern Norway. This tongue (up to <3‰ $\delta^{18}O$) matches spatially with cold SSTs deduced from foraminiferal counts [*Beyer*, 1987; *Schulz*, 1994; M. Weinelt, unpublished data, 1995]. When combined, these two lines of evidence indicate that the main cause of lowered $\delta^{18}O$ is dilution by isotopically light meltwater. Based on the distribution of low $\delta^{18}O$ values and especially on the fact that the region of minimum $\delta^{18}O$ values at 72°N would have been largely separated from the Atlantic in the south by a lowered sea level and a dried-up shelf, the main part of the meltwater appears to come from Norway, probably south of 68°N. We propose that iceberg flotillas originating from central Norway were the cause of the low-saline water tongue, whose drift pattern was influenced to an extent by the Lofoten Archipelago.

A similar pattern is observed in the earlier 55 ka time slice (author's unpublished data, 1994) that marks the end of the "termination" concluding glacial isotope stage 4. On the other hand, the 26 ka time slice is the last in a series of meltwater events that occur throughout isotope stage 3 [*Weinelt*, 1993]. These multiple meltwater events and their geographical distribution suggest that melting phases repeatedly affected both the Scandinavian and Greenland ice sheets after glacial stage 4 and within stage 3. Contrary to the major meltwater pulse at around 14.2-13.2 ka (see below), which shows its most prominent influence just west of the Barents Sea, the 26 ka event indicates most meltwater originating in Norway. This suggests that the Barents Ice sheet was not as large or did not exist as an ice sheet extending across the entire Barents Sea in isotope stages 4 and 3 as it did in stage 2 [*Elverhøi et al.*, 1992; *Vorren and Kristoffersen*, 1986]. If we consider the inferred counterclockwise thermohaline circulation at 26 ka, the surface circulation pattern of the Nordic Seas in principle remained similar to the present, even at these times of strong freshwater forcing on the surface circulation.

Within the precision of time control, the 26 ka time slice corresponds with Heinrich layer 3 in the North Atlantic [*Bond et al.*, 1992]. The documentation that various meltwater tongues originated from Scandinavia, Greenland, and the Arctic during H layer H3 is strong evidence that sudden meltings associated with H layers are not confined to the Laurentide ice sheet but are features that affect the other major northern hemisphere ice sheets as well. These results also agree with *Grousset et al.* [1993] who concluded that at least portions of Heinrich layer 3 in the North Atlantic originated from the Nordic Seas region, based on the distribution pattern of the IRD and its Nd/Sr isotope ratios. Our results constrain theories explaining Heinrich event 3 because the dynamics of an individual ice sheet can not be the only cause; there must be a multiregional mechanism within the climate system, such as eustatic sea level rises that could simultaneously trigger sudden deglaciations of different ice sheets.

The low $\delta^{13}C$ values, which approximately match the areas of low $\delta^{18}O$ (and low SST) values, suggest that meltwater blocked deep convection and led to a more pronounced pycnocline that increased the trapping of nutrients and served as favorite habitat of *N. pachyderma* (s), similar to the modern setting found in the Fram Strait (Figure 5b [*Carstens and Wefer*,

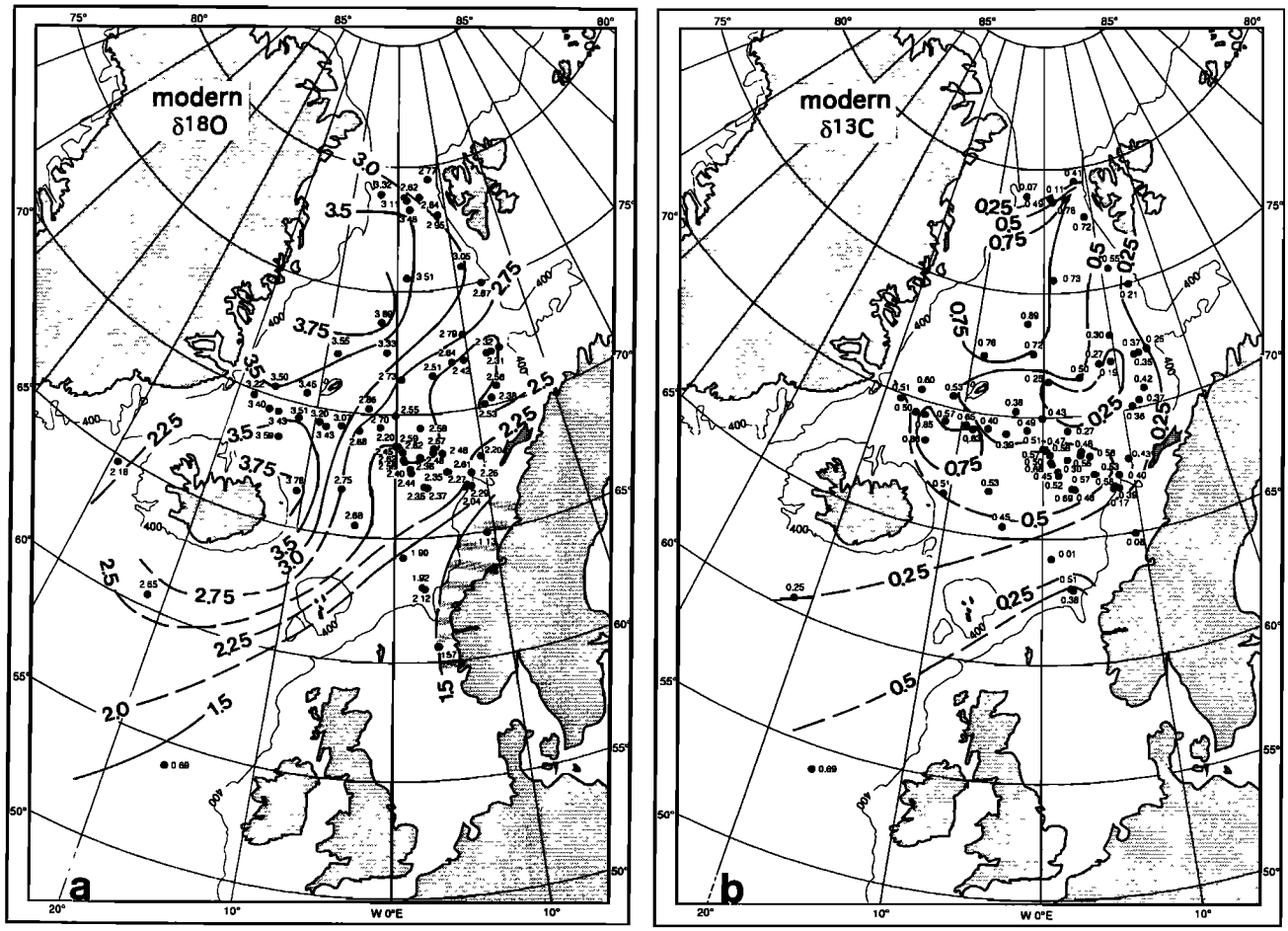

Figure 5. Distribution of modern (a) $\delta^{18}O$ and (b) $\delta^{13}C$ values in the Nordic Seas and NE North Atlantic. Horizontal hatching marks low salinity of Norwegian Coastal Current.

1992]). On the other hand, deepwater convection is apparent in the central gyre of the NGS at 26 ka. The extremes in low ventilation of North Atlantic surface water occur west of Ireland. They match a drastic reduction in benthic $\delta^{13}C$ in a number of cores from deep and intermediate water. This low in deepwater ventiation at the end of stage 3 is a phenomenon of global significance and suggests that the thermohaline circulation was strongly modified in the Atlantic [*Oppo and Fairbanks*, 1993; *Shackleton and Pisias*, 1985; *Beyer*, 1987; *Sarnthein et al.*, 1994].

The Peak Glacial

Isotopic distribution patterns. During the LGM, the northern North Atlantic was characterized by the marked contrast in the isotopic composition of the Atlantic surface water south of the Iceland-Scotland Ridge (which was ice-covered along about 50% of its length [*Wold*, 1992; *Sejrup* et al., 1994]) and the Norwegian-Greenland Sea (Figure 7). The Atlantic to the south showed both lowered $\delta^{18}O$ values of 4.0-4.1 ‰ and lowered $\delta^{13}C$ values of -0.2 to -0.4‰ east of about 20°W and higher $\delta^{18}O$ (>4.5‰) and $\delta^{13}C$ values (> -0.2‰) west of 25°W. By contrast, the Nordic Seas were marked by much higher isotopic values. Wide parts of the central Norwegian Sea display $\delta^{18}O$ values of 4.7-4.9‰, which extend to a long tongue stretching west of the Barents Shelf. Along the eastern margin this area of high $\delta^{18}O$ is bordered by a 100 km narrow "band" of water with slightly lower $\delta^{18}O$ values (4.3-4.5‰) adjacent to the Fennoscandian and Barents ice sheets.

Similar patterns and gradients apply to the carbon isotopes, with values of 0.15-0.25‰ in the central regions and values less than -0.01 to -0.15‰ along the eastern margin. Although the isotopic variability was generally subtle, the Greenland Sea data depict some small-scale patterns (consistent between cores) with a high in $\delta^{13}C$ and $\delta^{18}O$ extending northeast of Jan Mayen. To the north and southwest of Iceland, $\delta^{18}O$ and $\delta^{13}C$ are reduced. These values occur in a range similar to the eastern margin of the Nordic Seas. The Fram Strait and the marginal Arctic displayed heavy isotope values such as in the central Nordic Seas.

Discussion. The most striking feature of the last glacial maximum was the largely circular and uniform $\delta^{18}O$ maximum in the central Norwegian-Greenland-Sea, with two banana-shaped narrow maxima extending off middle Norway and west of the Barents Shelf margin. These structures reveal the glacial paleoceanography of the Nordic Seas in conjunction with the (few available) estimates of glacial summer SST (Figures 4 and 8) based on planktonic foraminiferal

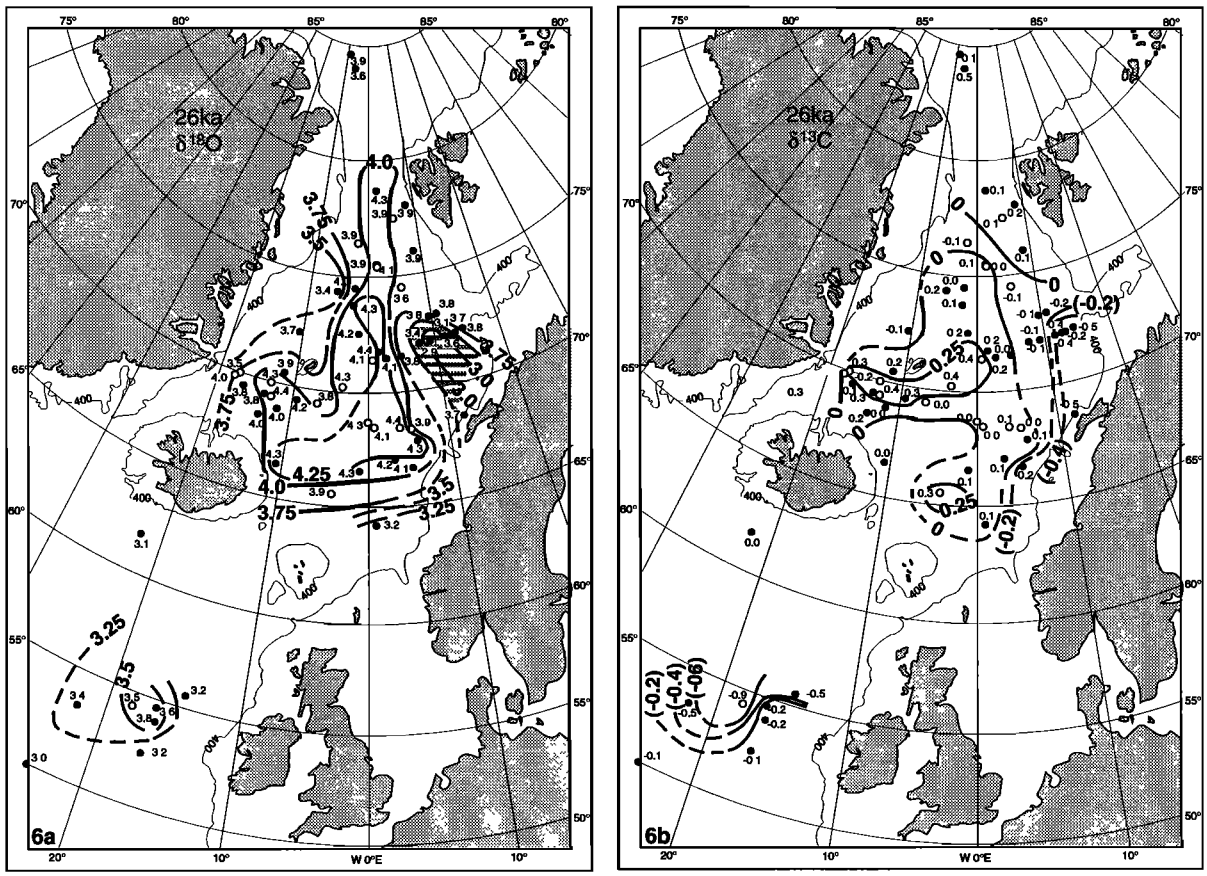

Figure 6. Distribution of (a) $\delta^{18}O$ and (b) $\delta^{13}C$ values in the Nordic Seas and NE North Atlantic at 26.0 ^{14}C ka. Horizontal hatching marks meltwater tongue.

assemblages [*Pflaumann et al.*, 1995, *Schulz*, 1994]. These estimates range uniformly near 3°-5°C since the beginning of glacial stage 2.

Contrary to assumptions of *Kellogg* [1980] and *Climate: Long-Range Investigation, Mapping, and Prediction (CLIMAP)* [1981] but in some ways in line with the early suggestions of *Olausson* [1972], the fairly well substantiated SST estimates of 3° to >4°C during glacial summers suggest that the glacial Norwegian-Greenland Sea and the Arctic off NE Greenland were at least seasonally ice-free. This is corroborated by the glacial $\delta^{13}C$ values as compared with the values of the modern perennially ice-covered central Arctic Ocean [*Spielhagen and Erlenkeuser*, 1994]. Here the values of *N. pachyderma* (s) (about 0.8-1.1‰) are in perfect equilibrium with the atmosphere and are much higher than in both the LGM Nordic Seas (-0.15 to 0.25‰) and in the modern, partially ice-free Greenland Sea (0.2-0.9‰ $\delta^{13}C$). Moreover, the LGM sedimentation rates at 67°-72°N strongly indicate an ice-free LGM Norwegian-Greenland Sea, because they are high and have concentrations of *N. pachyderma* (s) as high as during the Holocene (Figure 4). This is in contrast to the extremely low sedimentation rates found in the modern ice-covered Arctic.

In conclusion, various lines of evidence strongly suggest the absence of a permanent ice cover during the LGM. The unexpected open-sea conditions imply that using the CLIMAP reconstruction as boundary conditions for general circulation models (GCMs) of the LGM [*Manabe and Broccoli*, 1985; *Joussaume*, 1989; *Lautenschlager*, 1991] may introduce significant errors. Future modelling based on seasonally open waters in the Nordic Seas will be more realistic. Open-sea conditions may even hold true for the LGM Arctic north of Greenland up to 85°N (Figure 7a and recent data of *Stein et al.* [1994]) and provide an explanation for the large but short-term oceanic moisture supply needed to build up the huge Scandinavian, Barents Sea, and Svalbard ice sheets in the early to late LGM. A similar regime was proposed by *Veum et al.* [1992]. Based on maxima of *G. quinqueloba* in cores off Svalbard at 78°N, *Hebbeln et al.* [1994] also document possible intrusions of Atlantic water up to this latitude in the age range of the LGM.

The contours of the $\delta^{18}O$ maxima (>4.7/>4.8‰) indicate a two-gyre current pattern for the central-to-northern portion of the Nordic Seas (compare Figure 16b), a circulation that can be also inferred from the higher densities in the center of these gyres (deduced from high $\delta^{18}O$ values and SST of 3°-5°C; see below) and from the distribution of IRD [*Henrich*, 1992]. The LGM $\delta^{13}C$ values only reach about 0.25‰ and may correspond to about 1.1‰ in the modern ocean (assuming a deviation of *N. pachyderma* (s) values by -0.85‰ [*Labeyrie and Duplessy*, 1985], and 1.4‰, assuming a glacial atmospheric ^{13}C reduction of 0.3‰ [*Leuenberger et al.*, 1992]). Based on this low $\delta^{13}C$ level, we conclude that the ventilation of the Nordic Seas was less effective than in the modern Arctic water mass but better than in many parts of the modern and glacial Atlantic. Note the high glacial $\delta^{13}C$ values of *C. wuellerstorfi*

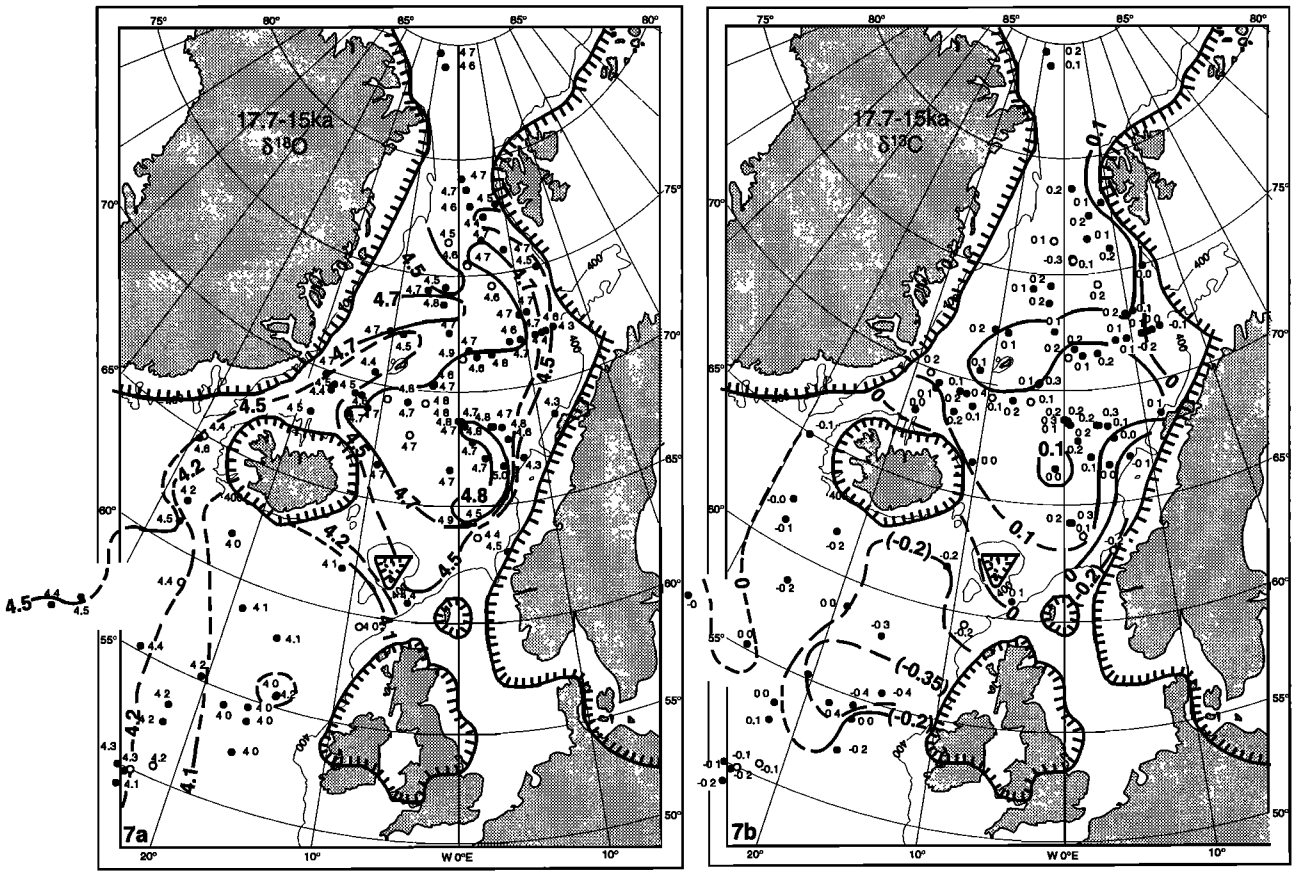

Figure 7. Distribution of (a) $\delta^{18}O$ and (b) $\delta^{13}C$ values in the Nordic Seas and NE North Atlantic during the LGM, 17.7-15.0 ^{14}C ka. Indented lines mark continental ice sheets [*CLIMAP*, 1981; *Elverhoi et al.*,1992; *Sejrup et al.*, 1994].

on the Rockall Plateau at 1400-1600 m depth, which reach about of 1.75‰ [*Sarnthein et al.*, 1994] and imply a deepwater source much different from the Nordic Seas.

The low planktonic $\delta^{18}O$ values west of Ireland (Figure 7a), which slowly increase toward the west Atlantic near 25°-30°W [*Keigwin and Boyle*, 1989], record a widespread salinity reduction in the LGM surface water. Here the salinity is estimated to have been 0.7-1.5 ‰ lower than in the Nordic Seas, when taking into account (1) the low glacial summer SSTs (4.4°-5.2°C south of Iceland; Figure 8) that were almost as low as at 67°-72°N and (2) the modern regression slope of 1‰ $\delta^{18}O$ versus 2‰ sea surface salinity (SSS). Typically, this water Because of Coriolis forcing, this lens of low-salinity surface water may have led to a paleogyre turning anticyclonic (clockwise) around Rockall Plateau and leading to a north-south flowing coastal current west of Ireland, possibly continuing down to Portugal [*Duplessy et al.*, 1991]. The origin of the freshwater is linked to melting iceberg flotillas. They produced frequent plough marks on the Iceland-Faeroe Ridge down to >700 m depth (F. Werner, personal communication, 1995) and came from the northwest Atlantic, as shown by the distribution of IRD [*Robinson et al.*, 1995]. In addition, icebergs possibly came from the Irish Sea [*Eyles and McCabe*, 1989].

The passages between the Nordic Seas and the open North Atlantic were strongly restricted because of (1) sea level lowering (the modern sill depth is 400-600 m), (2) extended ice sheets reaching the shelves of Shetland, Faeroe, and Iceland, and (3) the inferred iceberg flotillas congested west of the British Isles. Hence the water exchange was almost barred, which was particularly obvious from the steep isotopic gradients east and west of Faeroe (Δ 0.4-0.8 ‰ $\delta^{18}O$ and Δ 0.2-0.25 ‰ $\delta^{13}C$; Figure 7). In contrast to the east, the $\delta^{18}O$ pattern west of Iceland and planktonic foraminifera counts in core V28-14 suggest a distinct northward extension of the 4° warm paleo-Irminger Current (Figure 8). The current probably led to a marked incursion of Atlantic surface water into the Icelandic Sea, characterized by lower foraminiferal $\delta^{18}O$ values that extend from the Denmark Strait up to Jan Mayen and represent either lowered salinity and/or increased SST. Below this inflow a striking glacial maximum in benthic foraminifers (*Cassidulina teretis*) [*Struck*, 1992] records an increased local nutrient flux as found north of Svalbard today.

Deglacial Meltwater Events

Description. Similar to late stage 3, pronounced meltwater pulses mark the last deglacial in the Nordic Seas, though with markedly different isotopic distribution patterns that are probably the result of different source regions for major iceberg calving and of variations in currents and wind fields.

The time slice 14.2-13.2 ka (Figures 9a and 9b) shows the most extreme local $\delta^{18}O$ contrasts in the Nordic Seas ever observed over the last 60,000 years [*Weinelt*, 1993].

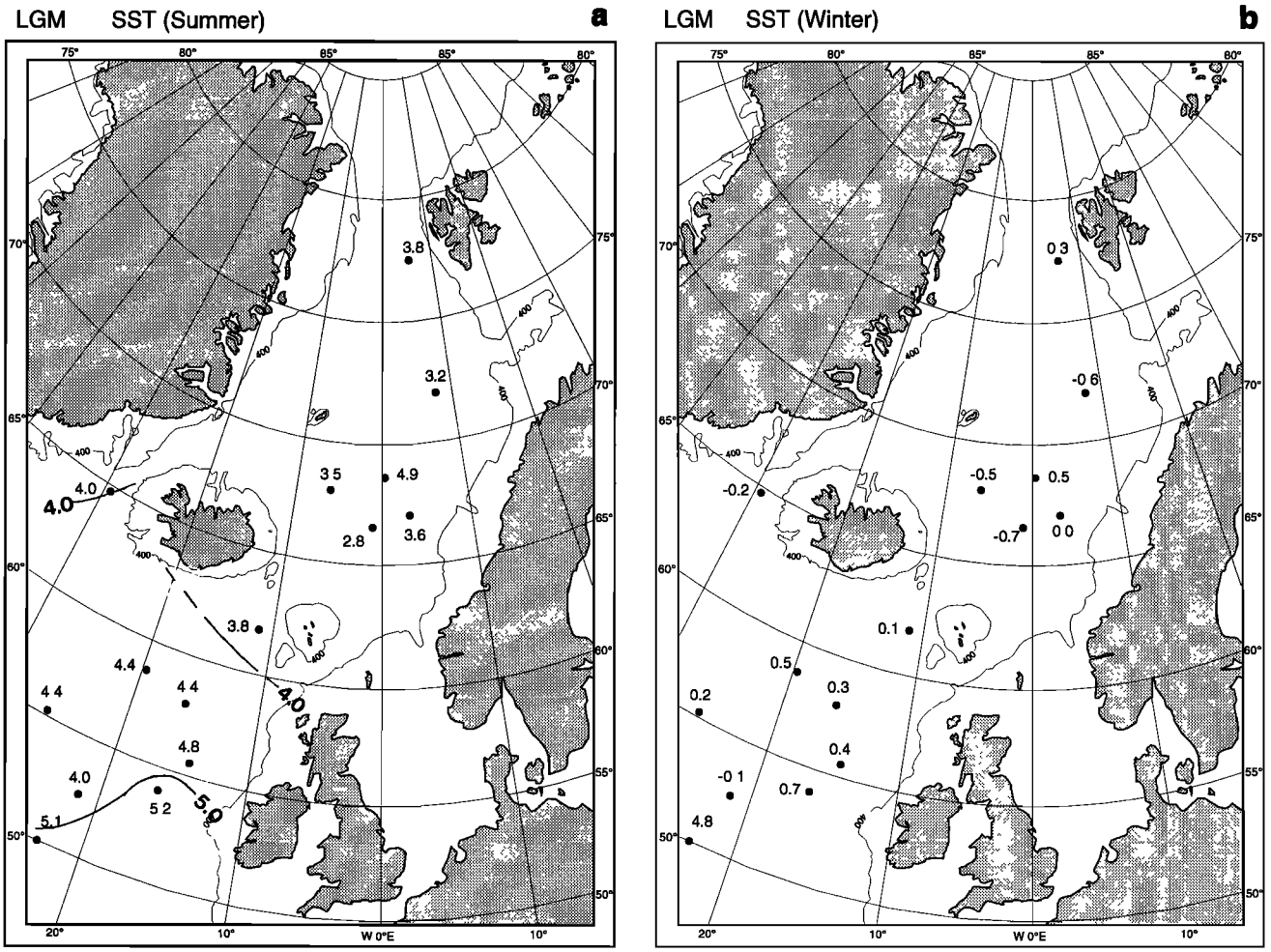

Figure 8. Reconstructed SST during LGM (a) summer and (b) winter.

1. A marked minimum tongue (2.6-2.8‰) extends from the Denmark Strait to Jan Mayen.

2. The most pronounced $\delta^{18}O$ minimum occurs in the northern Norwegian Sea (two good records with 1.6‰ in the center, six good records along the flanks), 180 km away from the LGM ice margin of the Barents Shelf. This $\delta^{18}O$ minimum does not extend northwest toward the Fram Strait. From north to south, however, a gradual $\delta^{18}O$ increase has led to two southward pointing lobes (based on seven good records).

3. A narrow $\delta^{18}O$ maximum of 4.0-4.12‰ crosses the Nordic Seas from east of Iceland up to the Fram Strait. This maximum is bordered on either side by extremely steep isotopic gradients of Δ1.3-2.5‰ $\delta^{18}O$ that document two sharp frontal systems running north-south. In the central North Atlantic a belt of low $\delta^{18}O$ values (2.35-2.6‰) stretches south-north from 50°N/25°W to southwestern Iceland. The $\delta^{18}O$ values increase toward the east by up to 3.1-3.4‰ west of Ireland and Scotland, which is different from the LGM. Thus the $\delta^{18}O$ minimum in the central Atlantic is clearly separated from the $\delta^{18}O$ minimum off northern Norway.

Low foraminiferal $\delta^{13}C$ values of -0.1 to -0.35‰ parallel the $\delta^{18}O$ minima along the eastern margin of the Norwegian Sea and north of Iceland, as well as south of Iceland. The maxima hardly exceed 0.2-0.3‰. Overall, the $\delta^{13}C$ distribution is fairly homogenous from 50° to 85°N.

As compared to 14,200-13,200 years B.P., the isotopic distribution patterns were radically different 12,400-12,100 years ago (Figures 9c and 9d), the next time slice with anomalously low $\delta^{18}O$ values. This later time slice is approximately synchronous with the first major meltwater pulse (mwp-1A) of *Fairbanks* [1989]. Two less extreme $\delta^{18}O$ minimum lobes emanated from both central Norway and the northern Barents Shelf, with a further minimum off SE Greenland. Outside of these features, the central water masses show $\delta^{18}O$ values (up to 4.22‰) that are slightly higher than 14.2-13.2 ka (up to 4.12‰) (this difference is more significant if considering the slight reduction in the global $\delta^{18}O$ ice effect near 12.2 ka [*Fairbanks*, 1989]). Thus the local $\delta^{18}O$ contrasts (Δ1.6‰) remained similar. As compared to the antecedent meltwater event, the small-scale local contrasts in $\delta^{13}C$ at 12.2 ka clearly increased to more than 1.1‰, with an extreme low of about -0.7‰ near the center of the $\delta^{18}O$ minimum plumes at the basin margin and values of more than 0.4‰ outside of the plumes, in the basin center. In summary, the isotopic patterns at 12.4-12.1 ka more closely resemble the patterns of the stage 3.1 meltwater event (Figure 6) than those in the 14.2-13.2 ka time slice.

Discussion. Foraminifera counts at 14.2-13.2 ka reveal very low summer SST estimates for glacial Termination IA, about 3°C in the eastern Norwegian Sea and about 4-5°C in

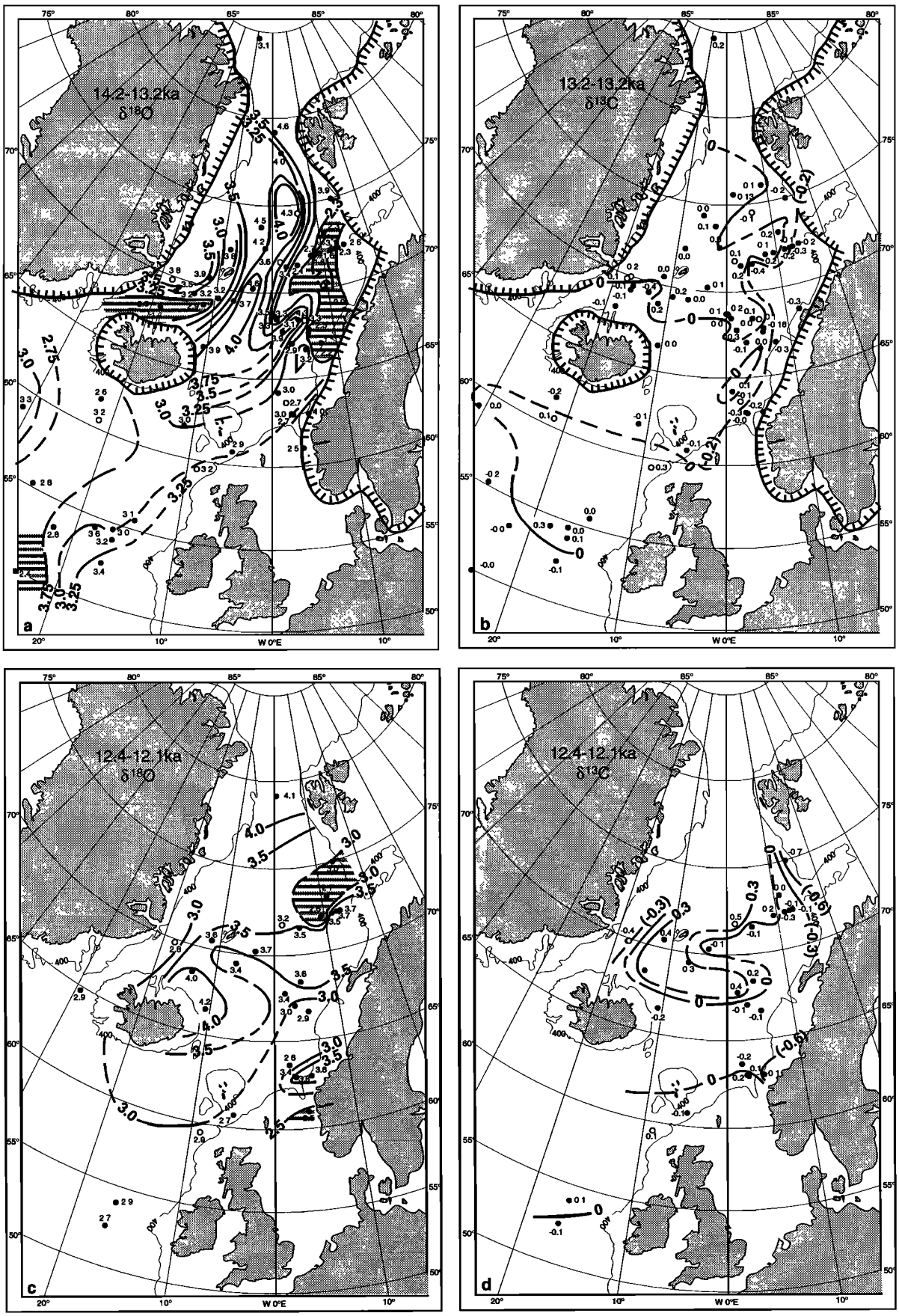

Figure 9. Distribution of $\delta^{18}O$ and $\delta^{13}C$ values in the Nordic Seas and NE North Atlantic during meltwater events, (a-b) 14.2-13.2 ^{14}C ka and (c-d) 12.4-12.1 ^{14}C ka. Indented lines in Figures 9a and 9b mark extent of LGM continental ice sheets to outline potential source areas of ice surges. Horizontal hatching in figures 9c and 9d marks meltwater tongues.

the Denmark Strait and west of Ireland (Figures 4 and 10). Based on diatom counts the SSTs in the far southeast of the Nordic Seas subsequently increase to 5°-6°C about 13.4-13.1 ka [*Karpuz and Jansen*, 1992]. In view of the low SST estimates about 13.6 ka, we interpret the pronounced $\delta^{18}O$ minimum centered near 72°N as a marked local salinity reduction of as much as 2.5-5.0‰ and of D1.5-3.0‰ for 12.4-12.1 ka (the range depends on the $\delta^{18}O$ of meltwater, i.e., the regression slope assumed for $\delta^{18}O$ versus SSS). We are thus confronted twice with major meltwater pulses from melting icebergs [*Weinelt et al.*, 1991; *Sarnthein et al.*, 1992].

The first and most pronounced case approximately corresponds in age to Heinrich layer 1 [*Bond et al.*, 1992, 1993). As shown in Figure 3, the melting off Norway started after 14.79-13.55 ^{14}C ka (cores 17730, 23071, and 23259). West of Ireland, however, in cores BOFS 5K, NA 87-22, V23-81, and ODP Site 609 [*Bond et al.*, 1992] it possibly started earlier, after 15.96-14.33 ^{14}C ka. Hence the Laurentide ice melt (HL1) may have involved an independent melting response on the Barents Shelf. The $\delta^{18}O$ pattern of this event clearly demonstrates that both the meltwater and the icebergs in the eastern Nordic Seas did not originate from the NW Atlantic [*Grousset et al.*, 1993] but from iceberg flotillas coming from a surging ice sheet on the Barents Shelf and melting only at some distance from the cold ice margin. In the time interval 12.4-12.1 ka, the pattern suggests that meltwater came to a larger extent from the North Sea, middle Norway, and probably also from south Svalbard.

At 14.2-13.2 ka, both the Coriolis forcing within the low-salinity/low-density water mass and its distinct outlines in the NE Nordic Seas, which appear barred toward the north and northwest but elongated to the south, suggest a local clockwise rotation (compare Figure 16c). Such a circulation would lead to a southward flow of cold water along Norway. If extending farther south, as some data points near Faeroe (cores CH 73-110, HM 1007, POS 16396) may indicate, this would promote a Europe wide cooling, such as the coeval Oldest Dryas [*Andrieu et al.*, 1993; *Lehman et al.*, 1991; *Karpuz and Jansen*, 1992]. Finally, one might predict to find a distinct (but as yet undiscovered) contribution of IRD from the eastern Norwegian Sea in northeast Atlantic sediments north of 55°N during later parts of Heinrich layer 1.

During the 14.2-13.2 ka event, summer SSTs between Greenland and Iceland were about 4.5°C (core V28-14 in Figure 4), i.e., about 1°-2° warmer than those west of Norway (near 3°C; Figure 10). These temperatures and the isolines to the south and north of Iceland suggest a "paleo-Irminger" inflow of relatively warm and less saline water (Δ 0.7-0.85‰

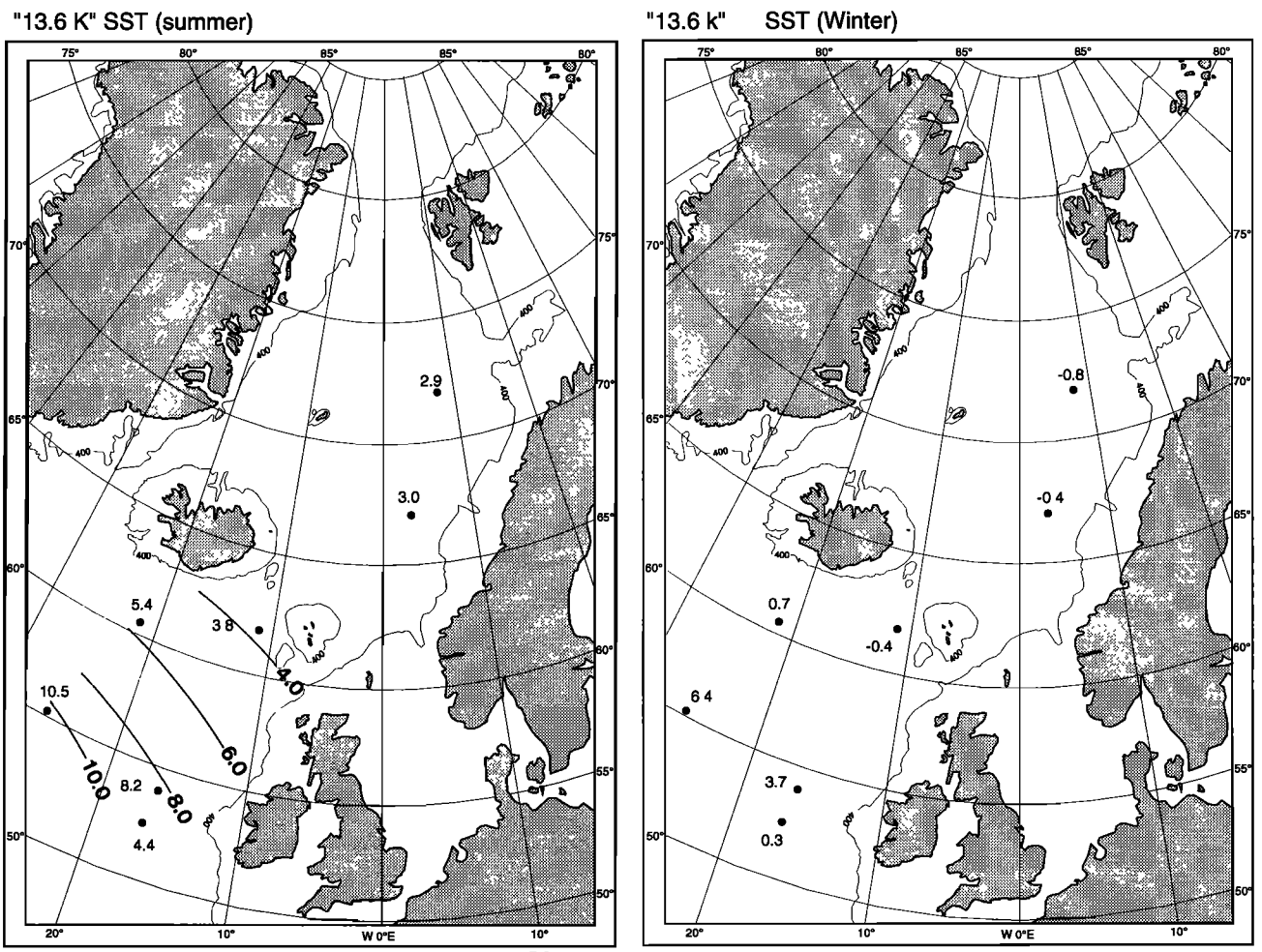

Figure 10. Reconstructed SST at the meltwater event about 13.6 ^{14}C ka.

$\delta^{18}O$) through the Denmark Strait and perhaps a cyclonic extension via Jan Mayen to the north. This centralwestern current may, in part, have carried meltwater from Iceland and Jan Mayen to the north, separated by a strong meridional frontal system from the higher-density water mass in the central Nordic Seas and by a second strong front from the anticyclonic gyre to the east. Fairly ubiquitous IRD, with Cretaceous *Inoceramus* debris in the Nordic Seas, ultimately originates from Cretaceous outcrops in the southeast [*Henrich*, 1992] and may further support the outlined model of a two-gyre surface circulation. These currents resulted in a very low diatom and foraminiferal productivity in the east and in the advection of both rare planktonic foraminiferal species [*Bauch*, 1993; H. Bauch, unpublished data, 1994] and first interglacial benthic species [*Struck*, 1992] from the open North Atlantic to the Icelandic Sea. Melting icebergs and strong density gradients, nevertheless, require an ice-free sea, at least, during summer. From the generally low and uniform $\delta^{13}C$ values we infer, together with the low salinities, a stop in deepwater convection, which is also recorded in Atlantic deepwater transects [*Veum et al.*, 1992; *Sarnthein et al.*, 1994].

In contrast to 14.2-13.2 ka (Figure 9b), the $\delta^{13}C$ gradients across the region at 12.4-12.1 ka (Figure 9d) were enhanced, with the maximum $\delta^{13}C$ values almost reaching 0.5‰. Hence the ventilation of the surface water was clearly strengthened in various parts of the Nordic Seas. Likewise, higher SST at the southeastern margin of the Norwegian Sea [*Karpuz and Jansen*, 1992] and higher densities NE of Iceland suggest a regime that permitted significant deepwater formation, also observed in the open Atlantic [*Sarnthein et al.*, 1994]. During this time interval the $\delta^{18}O$ distribution pattern with heavy values in the central Nordic Seas and light values along the margins was similar to the present. In summary, we infer a sluggish surface circulation that closely resembled the Holocene double cyclonic gyre south of 73°N.

Nonmeltwater Phases During the Last Deglaciation

Description. The oxygen isotopic values of the two deglacial time slices near 12.6-12.8 ^{14}C ka and the Younger Dryas (as defined above) show a Holocene-style meridional distribution pattern (Figures 11 and 5). There are only minor negative $\delta^{18}O$ deviations along the western (<3.8-4.0‰) and eastern margins (<3.2‰) as compared to the basin center (4.4-4.8‰). Due to the likely ^{14}C plateau near 12,700 ^{14}C years B.P. [*Lotter et al.*, 1992], the first time slice probably lasted significantly longer in terms of calendar years than indicated by the ^{14}C years (as outlined above).

As with $\delta^{18}O$, both time slices are characterized by lower $\delta^{13}C$ along the margins (-0.4-0‰ in the east and around 0‰ in the west) than in the central parts of the Nordic Seas (>0.3-0.6‰; Figure 11). Tongues of maximum values occur in the same central position as the present Jan Mayen current near 68°N; however, during the Younger Dryas they extend farther southeast into the Norwegian Sea than today. The low $\delta^{13}C$ values along the south Norwegian coast at 12.8-12.6 ka are contrary to what is observed during the Younger Dryas and present where the values rise (and finally decrease again in the Coastal Current). As today, lower $\delta^{13}C$ values follow in the Atlantic inflow (Figures 5b, 11b and 11d, [*Johannessen et al.*, 1994]). The average $\delta^{13}C$ level is almost as high as today, especially during the Younger Dryas which, in contrast to other past time slices, has high $\delta^{13}C$ values (0.25-0.6‰) west of Ireland, such as today (Figures 11d and 5b).

Discussion. These two time slices show isotopic distribution patterns that indicate a surface circulation differing little from the present current pattern. Important observations are that the meltwater influence was minor or absent and that the temperature estimates were low (Figures 4 and 12b). The two time slices correlate with the Oldest Dryas and the Younger Dryas cold spells, the latter confirmed by the identification of the Vedde ash layer.

Based on the cold SST estimates, the high $\delta^{18}O$ anomalies reflect both low temperature and high salinity in the Younger Dryas (Figure 12a), possibly a little lower than today (35.3 ‰). Within the accuracy of the summer SST estimates (Figures 4 and 12b), the $\delta^{18}O$ values of the central Nordic Seas, when corrected for the ice volume effect, indicate densities similar to present-day convective regions in the Iceland and Greenland Seas. The highest $\delta^{13}C$ has moved somewhat farther east than at present (compare Figures 11d and 5b). Hence convection may have extended much farther over the central Norwegian Sea than today and, perhaps, into the NE Atlantic. As with the SST, both the high $\delta^{13}C$ and $\delta^{18}O$ values indicate open waters during summer. On the other hand, the extremely low winter SSTs (Figure 12c) suggest a closed ice cover during winter and thus an extreme seasonality of climate.

During the Younger Dryas, two distinct tongues of heavy $\delta^{18}O$ values extended eastward SW of Jan Mayen Island and east of Iceland. These were similar but spread farther to the east than the modern (north) Jan Mayen and East Iceland currents that today advect polar waters in the Nordic Seas gyres (Figure 1). Different from today, they apparently did not carry less saline waters, as seen by $\delta^{18}O$ values that were higher than in other water masses of the Younger Dryas (Figure 11c). In summary, the two-gyre system of the Younger Dryas probably showed a strong extension of cold waters from west to east, which narrows the incursion of Atlantic waters from the south. Diatom evidence supports the narrow diameter of the Atlantic inflow corridor along the eastern margin [*Koc et al.*, 1993]. This zonal blocking, which is similar to the circulation pattern deduced for the Little Ice Age by *Lamb* [1977], is a potentially important mechanism in the Younger Dryas cooling of Northern Europe.

Although the import of heat, and possibly of salinity, was less important and seasonally interrupted in the Younger Dryas and 12.6-12.8 ka time slices than today, our reconstructions clearly suggest a surface inflow of Atlantic water and a thermohaline circulation pattern not unlike the modern. This contradicts earlier contentions that the onset of coolings was either linked with or caused by a stop in Nordic Seas thermohaline circulation [*Broecker et al.*, 1985a; *Broecker and Denton*, 1989; *Lehman and Keigwin*, 1991] and is in support of views suggesting that a modern type conveyor-belt circulation and deepwater formation prevailed in the cold spells [*Jansen*, 1987; *Jansen and Veum*, 1990; *Charles and Fairbanks*, 1992; *Labeyrie et al.*, 1992; *Veum et al.*, 1992; *Sarnthein et al.*, 1992, 1994]. Based on Atlantic deepwater $\delta^{13}C$ patterns the conveyor belt was probably a little less extensive than today but more vigorous than at the LGM and, especially, than during meltwater events [*Jansen and Veum*, 1990; *Veum et al.*, 1992; *Sarnthein et al.*, 1994]. Hence we are faced with a situation that coolings also appear to occur in situations with meridional circulation of some magnitude and active convection, posing an enigma for climate modelling.

The meridional type of circulation in the Younger Dryas also agrees with land evidence from Norway and Scotland showing a rather maritime climate with prevailing SW winds [*Larsen et al.*, 1984; *Sissons*, 1980], possibly reaching up to

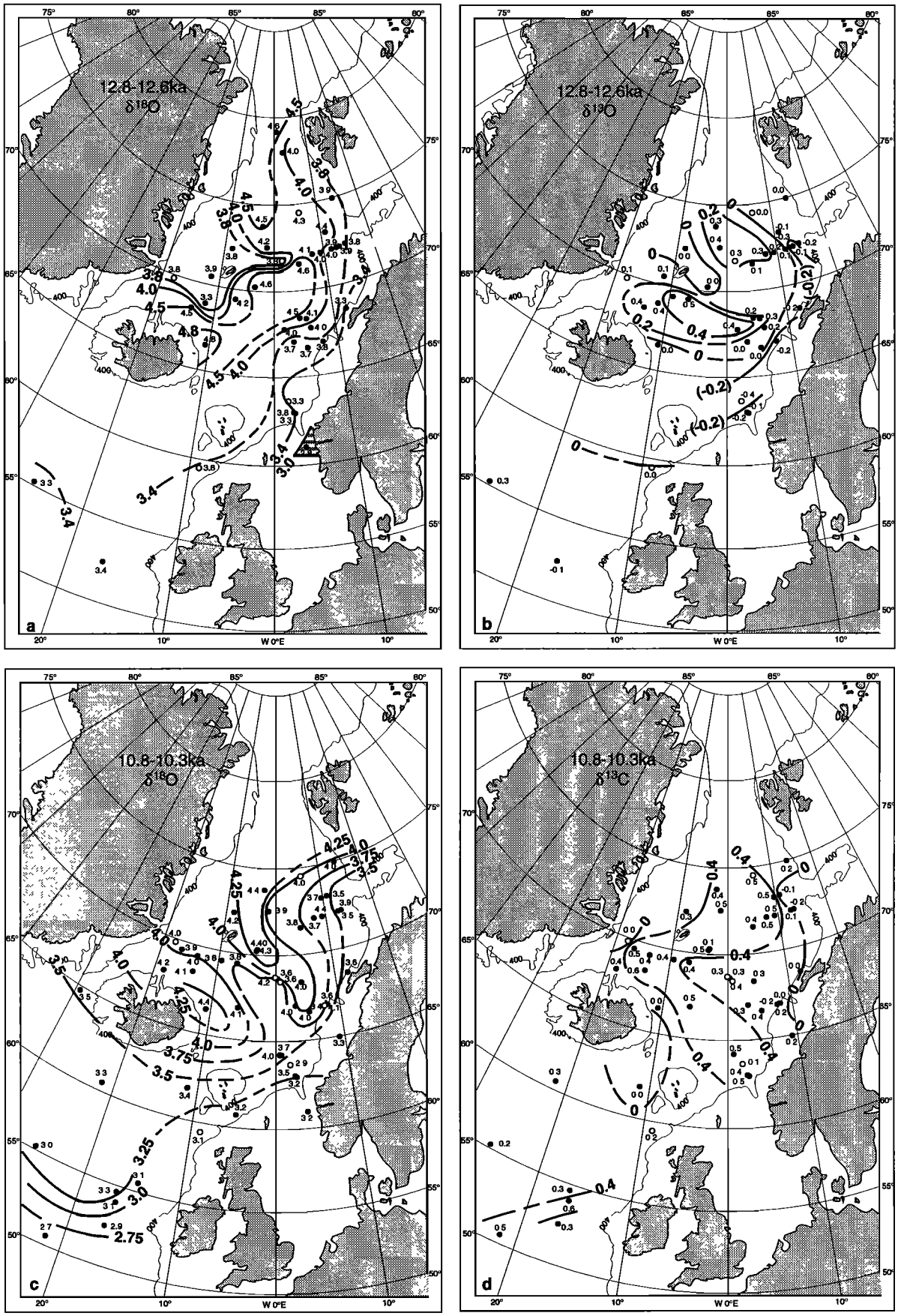

Figure 11. Distribution of $\delta^{18}O$ and $\delta^{13}C$ values in the Nordic Seas and the NE North Atlantic during non-meltwater phases at Termination I: (a-b) 12.8-12.6 ^{14}C ka; (c-d) 10.8-10.3 ^{14}C ka.

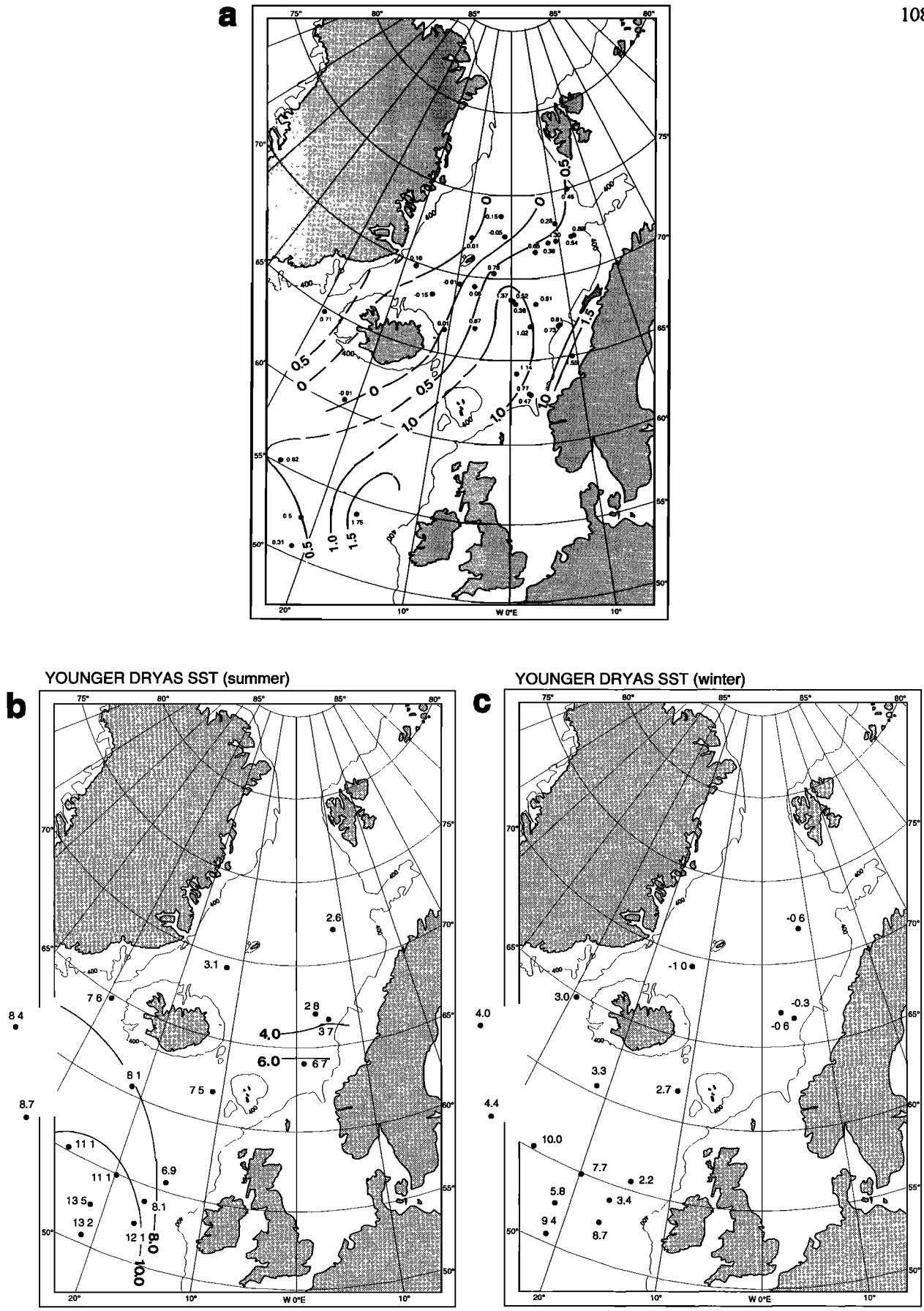

Figure 12. (a) Younger Dryas $\delta^{18}O$ anomalies versus present (difference between values in Figures 5a and 11a; ice volume effect of 0.63‰ [*Fairbanks*, 1989] subtracted. (b-c) Reconstructed SST in the Younger Dryas during summer and winter.

73°N. In conjunction with the lack of evidence for any large Younger Dryas ice advance on Spitzbergen [*Mangerud and Svendsen*, 1992], our evidence of more zonality in SST would imply that the (summer ?) atmospheric patterns also were more zonal, hence shielding the higher latitudes from receiving enough moisture to enhance snow accumulation at times of maximum summer insolation about 12,000 calendar years ago.

As for the Younger Dryas cold spell itself and its onset, the oceanographic mechanisms that controlled the end of the Younger Dryas in the Nordic Seas remain obscure. The final deglaciation on southeast Svalbard "timely" started at 10.37 ka [*Landvik et al.*, 1992; *Mangerud and Svendsen*, 1992] such as elsewhere in North Europe but without leaving any corresponding signal in the high-resolution $\delta^{18}O$ records measured in nearby sediment cores. Possibly, there was a small local meltwater lens that hid the Younger Dryas cooling in the $\delta^{18}O$ curves indistinguishably from the subsequent strong warming which is documented in planktonic faunal and Uk37 records [*Koc et al.*, 1993; *Schulz*, 1994; *Rosell-Melé*, 1994]. In the benthic fauna and stable isotopes from the southern Barents Shelf the Younger Dryas also is poorly recorded [*Steinsund et al.*, 1991; *Hald et al.*, 1991].

Intra-Holocene Variability

Description. The three Holocene time slices at about 9 ka, 6.5 ka, and "modern" (Figures 13 and 5) depict largely constant $\delta^{18}O$ and $\delta^{13}C$ values and a consistent zonal and meridional distribution pattern. Minor deviations only occurred in the earliest Holocene where some lighter $\delta^{18}O$ and $\delta^{13}C$ values along the eastern margin of the Nordic Seas deviate from the modern isotopic patterns. Based on low SST values (Figure 4) these local low $\delta^{18}O$ values suggest a reduced salinity and hence a final supply of meltwater, especially north of 72°N. West and south of Iceland, constant $\delta^{18}O$ values in conjunction with warming SSTs suggest that the salinity of the Irminger Current reached a maximum near 6 ka and decreased somewhat over the last few thousand years (cores V28-14 and SU 90 108 in Figures 3 and 4). The $\delta^{13}C$ values increased slightly in the Icelandic Sea from 0.6 to 0.7‰ in the early Holocene to >0.8 ‰ during middle and late Holocene times (Figures 13 b, 13d, and 5b).

Discussion. Based on the three time-slice reconstructions (Figures 5 and 13), the Holocene generally appears as a period of long-term stability in ocean climate, without major evolutionary trends and/or important short-term events, a result that is in harmony with the Greenland ice core record [*Dansgaard et al.*, 1993]. This stability strongly contrasts with the marked short-term variability of climate during stage 3 [*Weinelt*, 1993] and Termination I. The cessation of early Holocene meltwater input from the eastern margin, a slight mid-Holocene increase in salinity and late Holocene decrease in SST of the Irminger current, and a middle Holocene increase in $\delta^{13}C$ and surface-water ventilation of the Icelandic Sea form the only signs of modest change. No changes are found in the meridional advection of Atlantic water into the Norwegian Sea and in the zonal advection of cold water north of Iceland and Jan Mayen, changes that may be compared with Younger Dryas-style patterns. On the other hand, the diatom record [*Koc et al.*, 1993] documents that the polar waters spread farther eastward in the Greenland and Iceland Seas after about 6 ka, indicating a late Holocene response to the decreasing solar insolation in the Holocene. Short-term variations such as the Little Ice Age are not resolved in our sedimentary records.

The apparent uniformity of the composition of surface-water masses implies a largely constant formation of deep water in the Nordic Seas, as is shown in deepwater reconstructions of the Atlantic [*Sarnthein et al.*, 1994].

General Discussion

Modes of Surface Water Circulation

In total, nine time-slice reconstructions (Figures 5-13) enable us to group the distribution patterns of surface water masses in the NE Atlantic and Nordic Seas into three different circulation modes (derivation of paleocurrent tracks and directions defined in the methods and strategies section).

The present interglacial/Holocene mode (Figures 5, 13, and 16a) is marked by cyclonic gyres, the northward advection of warm water along the northwest European shorelines from Ireland up to Svalbard, and a north-south flow of cold water that dominates the East Greenland margin. This circulation mode has apparently continued for the last 12.8 ^{14}C kyr (Figure 11a), that is, since prior to the Bölling, though the heat transport was much reduced in the beginning. This mode also includes the Younger Dryas (Figure 11) cold spell and significant meltwater plumes, the origins of which are linked to both the Scandinavian and Greenland ice sheets, for example, at the end of $\delta^{18}O$ stage 3 (Figure 6) and the Bölling (Figure 9c). During these times (moreover, at the beginning of stage 3 [*Weinelt*, 1993]), the distribution of meltwater lenses suggests a current flowing south-north off Norway, which is deflected to the northwest by the promontory of the Lofoten Archipelago. Since the meltwater tongue off Norway at 26 ka is coeval with Heinrich event 3 [*Bond et al.*, 1992, 1993], the Laurentide ice sheet was probably not the only major meltwater source in high latitudes during this time.

The second major mode of North Atlantic surface circulation is linked to the LGM. Characteristic of this mode is the cessation of surface-water transport northward across the eastern Iceland-Faeroe ridge, whereas the paleo-Irminger Current apparently extended farther north into the Icelandic Sea. The glacial Nordic Seas were probably ice-free, at least during summer, and showed a persistent Holocene-style anticlockwise current pattern. West of Ireland, melting icebergs led to a widespread reduction in sea surface salinity (Figures 7 and 8a) and possibly induced a weak clockwise gyre. This striking feature may have diverted the warm North Atlantic Drift water away from Western Europe and the central Atlantic toward Iceland in the north, which involves an additional cooling for Europe during the LGM (Figure 16b).

Comparison of the Younger Dryas conditions (within mode 1) with the LGM mode 2 shows both similarities and differences. In both cases we find lower isotopic values along the margins of the Nordic Seas and higher values in the center, suggesting cyclonic gyres, some meridionality, and seasonally open waters. In the northeast Atlantic sector, however, the Younger Dryas appears much more meridional, as shown by SST estimates which are, at least, 5°C warmer than during the LGM (Figure 7), when the influx of Atlantic water appears to be barred in the Faeroe region. On the Barents Shelf and Svalbard, the rapid growth of the LGM ice sheets may reflect open waters and a meridionality of circulation in the northern Norwegian Sea at the LGM. Here the combination of lower summer insolation/higher winter insolation and lower sea level evidently made ice growth possible at the LGM, whereas the Younger Dryas, with currents that were more meridional in the south and provided ice growth in Scandinavia and Scotland,

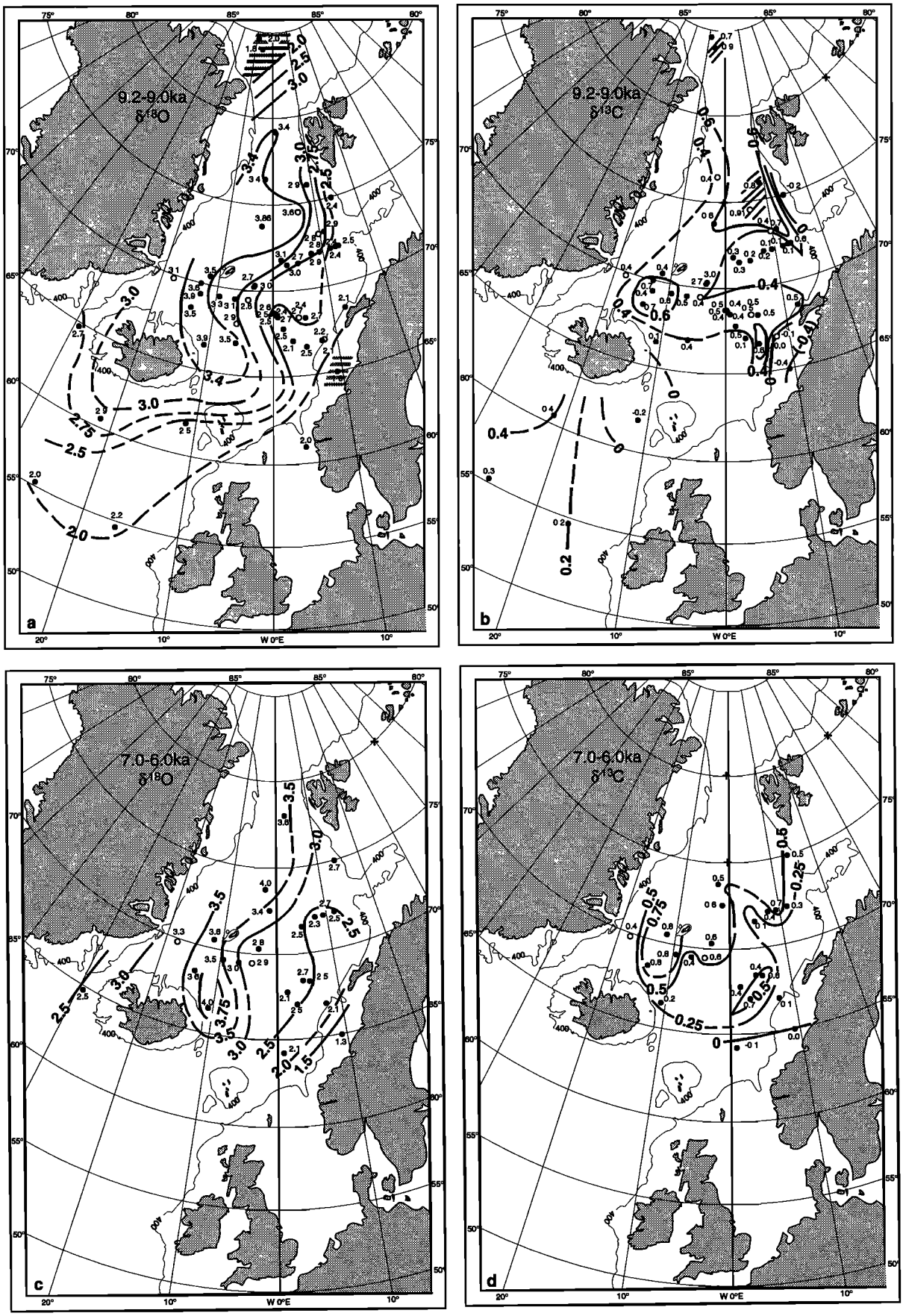

Figure 13. Distribution of $\delta^{18}O$ and $\delta^{13}C$ values in the Nordic Seas and northeast North Atlantic: (a-b) 9.0 ^{14}C ka; (c-d) 6.5 ^{14}C ka. Horizontal hatching marks low salinity of Norwegian Coastal Current.

did not supply enough moisture to sustain ice growth in the Svalbard region where summer insolation and sea level were much higher than during the LGM.

The third circulation mode occurred during the first meltwater event subsequent to the LGM, approximately synchronous with Heinrich event 1 [*Bond et al.*, 1992, 1993] or a few hundred years later. This mode deviated most strongly from the Holocene pattern with a small gyre that probably turned anticyclonic/clockwise. This prominent circulation feature persisted west of Norway (Figures 9 and 16c) over almost 1000 years. Based on our reconstructed patterns, the gyre was induced by a giant meltwater lens derived from icebergs coming from the surging ice sheet on the Barents Shelf, which moved cold water far to the south and up to the far northeastern sector of the North Atlantic (Figure 9a) [*Weinelt et al.*, 1991; *Sarnthein et al.*, 1992]. Thus the meltwater producing Heinrich event 1 may not only have stemmed from the Laurentide/Inuitan ice sheets in the NW Atlantic but also from the northeast from ice on the Barents Shelf.

During this time, the far northward incursion of the Irminger current presents a strange feature in the Icelandic Sea, in contrast to a north-south flow previously assumed by *Keigwin et al.* [1991] and *Grousset et al.* [1993]. This extension of the Irminger current off Greenland was separated from the uncommon meltwater lens off Norway by two marked frontal systems running south-north across the central Nordic Seas (Figure 10a). In contrast to the LGM mode, the water exchange across the Iceland-Faeroe Ridge was fully reestablished during the meltwater event, possibly a few hundred years earlier (core HM 1007; figure on electronic supplement).

Surface-Water Density and Deepwater Formation

Paleodensity estimates were deduced as described in the methods and strategy section. Today the salinity and density of surface water are sufficiently high at many sites in the central Nordic seas to produce North Atlantic Deep Water (NADW) by a simple cooling of surface water down to <2°C (Figure 14a). Both to the west of Iceland (core V 28-14) and in the Norwegian Sea the densities of LGM surface water reach 28.2 to 28.4 g cm^{-3} at 3.6°-4.4°C during summer (Figure 14b). When cooling down to -1.5°C during winter (i.e., to the temperature of modern Norwegian Sea Deep Water (NSDW)), this surface-water density (including an error of ± 0.35 s_{ST}) may be almost adequate to form the glacial NADW the theoretical density of which is about 28.75 g cm^{-3} (Figure 14b, [*Labeyrie et al.*, 1992]).

The high paleodensities of the LGM surface water in the Nordic Seas parallel moderately high $\delta^{13}C$ values of *N. pachyderma* (up to >0.25‰ $\delta^{13}C$ versus modern values of 0.6-0.9‰), which reflect a modestly good ventilation. South of Iceland, however, the LGM densities (27.2-27.6) reach a minimum, and the LGM $\delta^{13}C$ values are as low as -0.2 to -0.4‰ (Figure 7). Here a persistent meltwater lens led to stratification and a ventilation low of the near-surface water. This area can thus be excluded from the potential source regions of glacial NADW, a water mass with benthic $\delta^{13}C$ values of 1.75‰ (equal to 0.9‰ for *N. pachyderma* (s)) at 1400-1600 m depth [*Sarnthein et al.*, 1994]. Based on the LGM paleosalinity distribution of *Duplessy et al.* [1991], the major site of glacial deepwater formation may be expected somewhere west of 25-40°W, outside of the study area and possibly in the Labrador Sea.

During circulation mode 3, which is linked to the high meltwater supply associated with Heinrich event 1, the site of relative maximum densities (27.0-27.4) and the highest ventilation rates of North Atlantic surface water moved east, to the west of the British Isles (3.0-3.45‰ $\delta^{18}O$, low SSTs, 0.1-0.28 ‰ $\delta^{13}C$; Figures 9 and 10). This low density, however, was insufficient to drive any significant intermediate water and deepwater formation [*Sarnthein et al.*, 1994]. During the subsequent pre-Bölling (12.8-12.6 ka), high surface water densities (27.8-28.0 g cm^{-3}) and a Holocene-style deepwater formation abruptly returned to the Nordic Seas, a feature which persisted until today, at least, until the end of the Younger Dryas, when a further short-term interruption may have occurred [*Sarnthein et al.*, 1994].

Impact on Climate of the Northern Hemisphere

In summary, it appears from our data that some meltwater events such as those at the end of stage 3 and near 14.2-13.2 ka led to a breakdown in deepwater formation and of the Atlantic Salinity Conveyor Belt, whereas other events such as that near 12.4-12.1 ka had little impact on surface-water paleodensity and deepwater formation in the North Atlantic.

When projected on a "Milankovitch" insolation record of the last 80 kyr (Figure 15), there were many meltwater events in the Nordic Seas and North Atlantic [*Broecker et al.*, 1992; *Bond et al.*, 1993; *Weinelt*, 1993] with the potential to act as a trigger for major climatic change: (1) During times of increasing summer insolation such as immediately subsequent to both stage 4 and the LGM, the density distribution and current regime of the meltwater events may have led to a major delay of the deglaciation of the northern hemisphere, such as during the Oldest Dryas. (2) During times of decreasing insolation such as near the end of stages 5 and 3, about 79 ka (documented by *Köhler* [1991] and M. Weinelt (unpublished data, 1993)) and near 26 ka, meltwater events could possibly induce a greatly accelerated cooling and thereby a possible mechanism to explain the hitherto little understood abrupt buildup of huge ice sheets on the northern continents. In summary, these events may form the "missing link" between the gradual effect of Milankovitch climatic forcing and the abrupt advance of large-scale continental glaciations actually observed, such as in Scandinavia [*Larsen et al.*, 1987; *Mangerud*, 1991] and the Alps [*Fliri et al.*, 1970].

The strong iceberg/oceanic meltwater influence from the Norwegian coast at 26 ka (Figure 6) demonstrates that the ice margin had advanced significantly enough to reach the shelf areas before 26 ka, suggesting a fast ice growth phase after the Ålesund interstadial about 30 ka [*Larsen et al.*, 1987; *Mangerud*, 1991]. During this time, the ice margin had been located inshore in western and northern Norway [*Mangerud and Svendsen*, 1992; *Sejrup et al.*, 1994, S.E. Lauritzen, personal communication, 1992], with fossil fish remains indicating a far reaching influx of Atlantic water [*Larsen et al.*, 1987]. It is unclear, however, whether the 26 ka meltwater event, which occurred only after the ice sheet again overrode the coastal areas, reflects a further short-term breakup of marine portions of this ice [*Mangerud*, 1991] or rather a further advance and surge prior to the LGM. However, the crucial trigger of the abrupt LGM cooling of Central Europe may be found elsewhere, as we surmise, along with the inferred iceberg flotillas stemming from Laurentia [*Robinson et al.*, 1995] and melting west of Ireland (Figure 7).

During the LGM, pollen records from ice-free areas on the outer coast of northern Norway (Andøya) document intervals marked by vegetation, which indicate maritime floral components and summer warmth [*Vorren et al.*, 1988; *Alm*, 1993], especially during ameliorated phases near 18,300-16,600 and

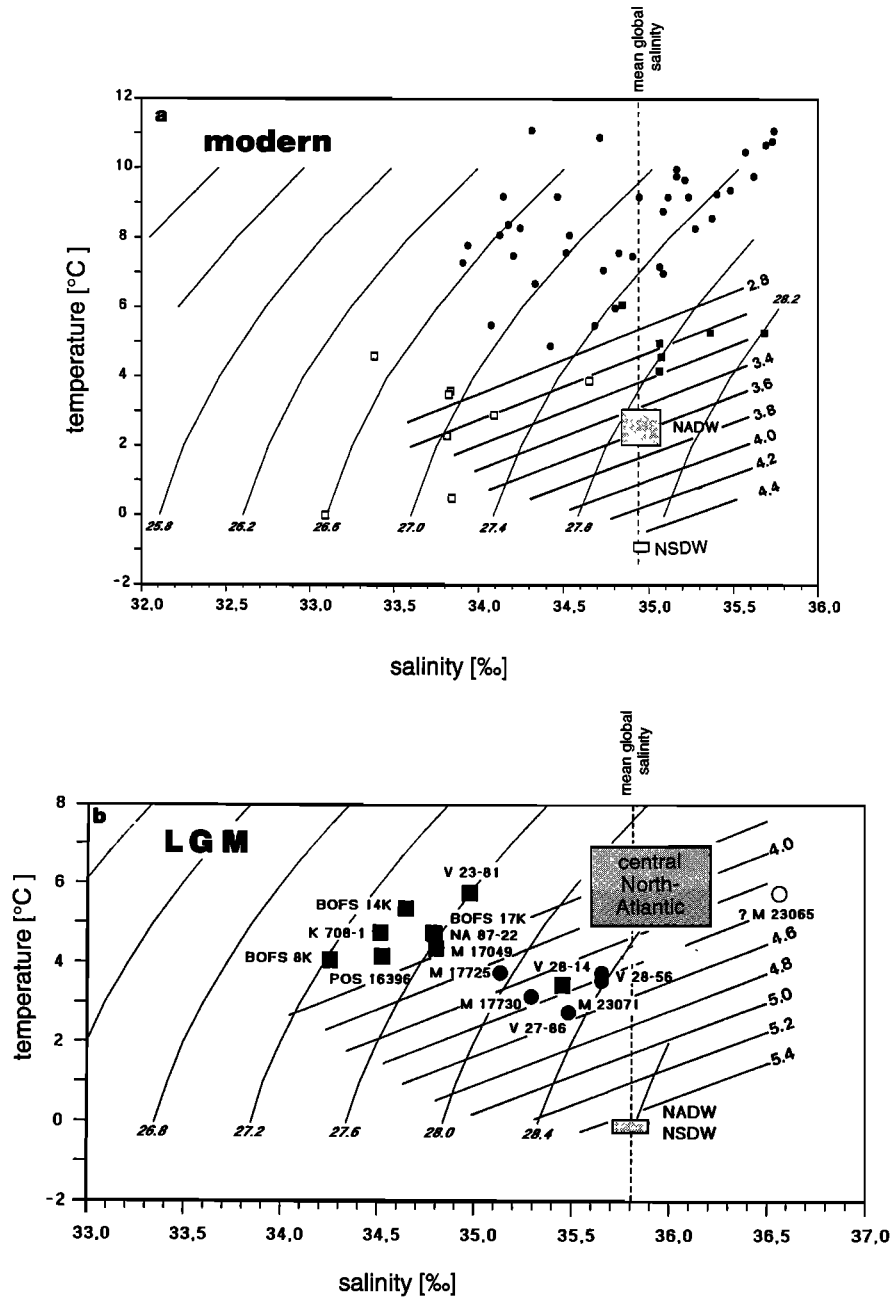

Figure 14. Sea surface temperatures (SST)/salinity/density diagram after *Cox et al.* [1970] and *Labeyrie et al.* [1992] for (a) modern and (b) last glacial maximum (LGM) surface water masses as defined by their $\delta^{18}O$ composition. SSTs for summer are deduced from planktonic foraminifer assemblages [*Schulz*, 1994]. Sea surface salinity is derived from $\delta^{18}O$ values (2:1) after correction for ice effect [*Fairbanks*, 1989] and SST. In Figure 14a, solid circles are samples below the Norwegian Current; solid squares are Arctic water mass; open squares are Polar water mass. In Figure 14b, solid circles are samples from the Nordic Seas; solid squares are from the NE North Atlantic.

16,000-15,000 ^{14}C years B.P. [*Alm*, 1993]. This supports our evidence for a seasonally ice-free sea and a distinct meridional component of the surface circulation. The open waters and northward movement of surface waters along middle and northern Norway may have promoted the rapid LGM growth of excess ice on the Barents shelf in two ways: (1) by acting as a moisture source and (2) by acting as a means for directing low-pressure cyclones with moisture to the far north, a process supported by strong land-sea contrasts.

As compared with other meltwater events such as at 55 ka [*Weinelt*, 1993, and own unpublished data, 1994] and 26 ka (Figure 6) the pronounced meltwater event following stage 2 at 14.2-13.2 ka (Figure 9a) appears unique: both the $\delta^{18}O$ distribution pattern and the absolute $\delta^{18}O$ values suggest that

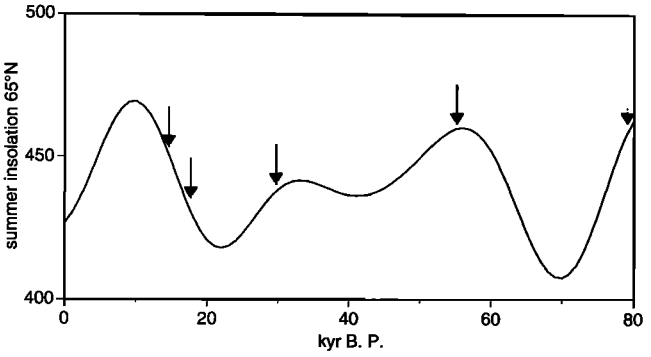

Figure 15. Summer insolation curve at 65°N [*Imbrie et al.*, 1984]. Arrows show major meltwater events. Arrows at 79 ka based on *Köhler* [1991] and at 55 ka on authors' unpublished data and *Bond et al.* [1993]. NSDW is the Norwegian Sea Deep Water. Ages in calendar years.

the deglaciation after the LGM was most prominent in the Barents region, indicating a much larger Barents ice sheet in stage 2 than in stage 4. This first deglacial meltwater event happened well before any significant warming and possibly led to a delay in the deglaciation of the neighboring continent. The first warming of a corridor along the coast of south Norway took place only near the end of the meltwater event at 13.4-13.2 ^{14}C ka [*Karpuz and Jansen*, 1992; *Koc et al.*, 1993; *Schulz*, 1994]. Similarily, a slight onshore warming occurred only after the Oldest Dryas cold spell, between 13.0 ^{14}C ka and the pronounced warm phase of the Bølling after 12.7 ^{14}C ka [*Paus*, 1989, 1990; *Andrieu et al.*, 1993] (synthesis by *Kaiser* [1993]). Accordingly, the warming happened after the meltwater influence had vanished and the meridional and conveyor-belt circulation were reestablished (Figure 11c). Subsequent glacier readvances as recorded in Scandinavia (12.3(?)-12.0 ^{14}C ka) may be responsible for the meltwater influence seen in the corresponding time slice (Figure 9c). A coeval cooling is documented in both marine diatoms [*Karpuz and Jansen*, 1992] and onshore pollen records (cool summers [*Paus*, 1989, 1990]). The subsequent Allerød deglaciation is hardly recognized in the oceanic δ^{18}O pattern and shows little meltwater influence (unpublished own data, 1994).

There are still problems in defining the precise chronology of the last deglacial, especially because of the ^{14}C plateaus [*Lotter et al.*, 1992]. In summary, our evidence reveals that the meltwater events could have induced coolings, most markedly during the great event at 14.2-13.3 ka. On the other hand, minimum meltwater influence, meridional circulation, and warming are characteristic of the Bölling-Allerød "type" climatic ameliorations.

Cooling also occurred during the Younger Dryas when meltwater influence appears minimal. This cold spell was characterized by meridional circulation with northward

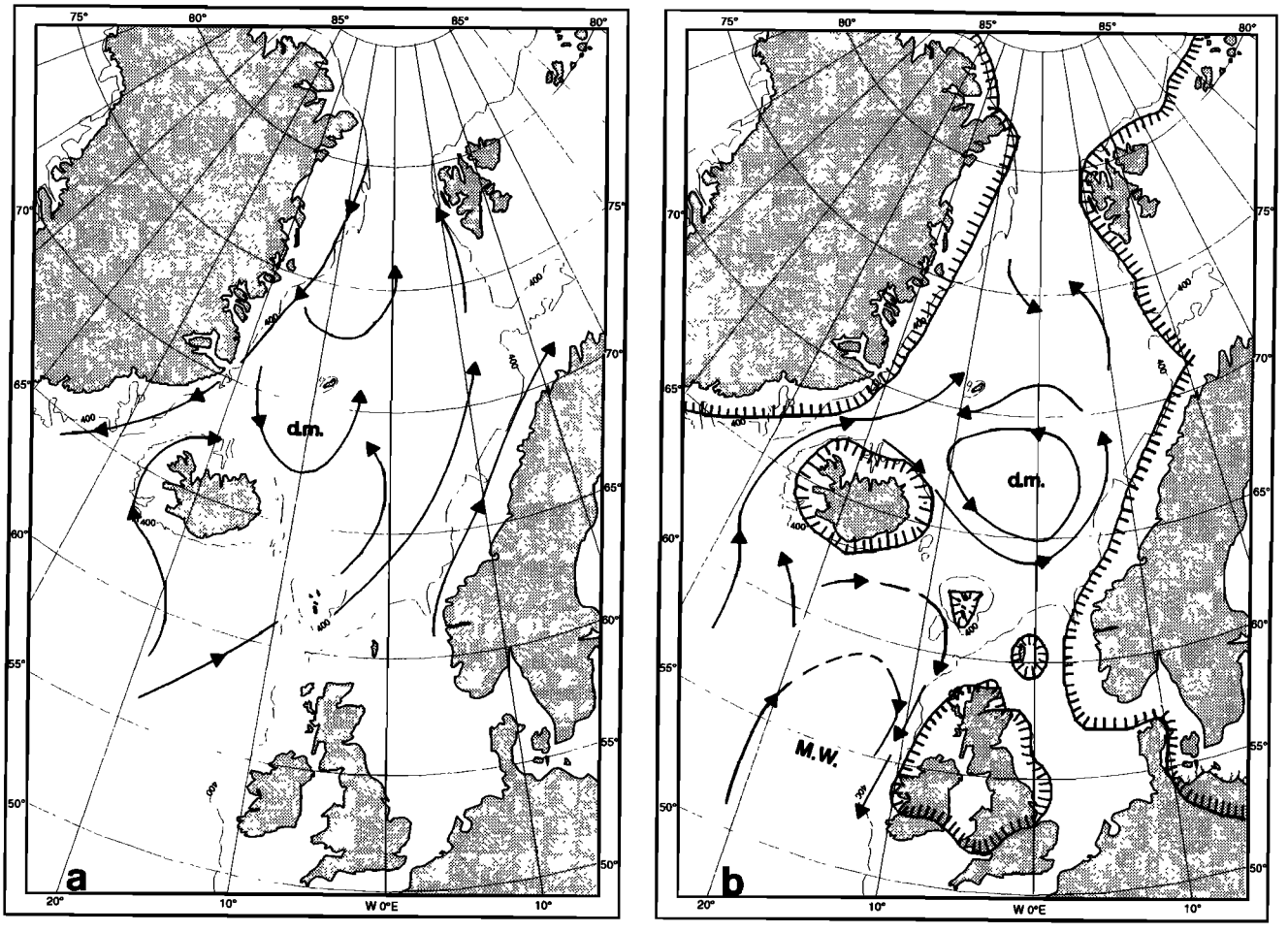

Figure 16. Paleocurrent directions as deduced from paleodensity gradients: (a) modern, (b) LGM, (c) 14.2-13.2 ka (M.W., meltwater); d.m. is density maximum.

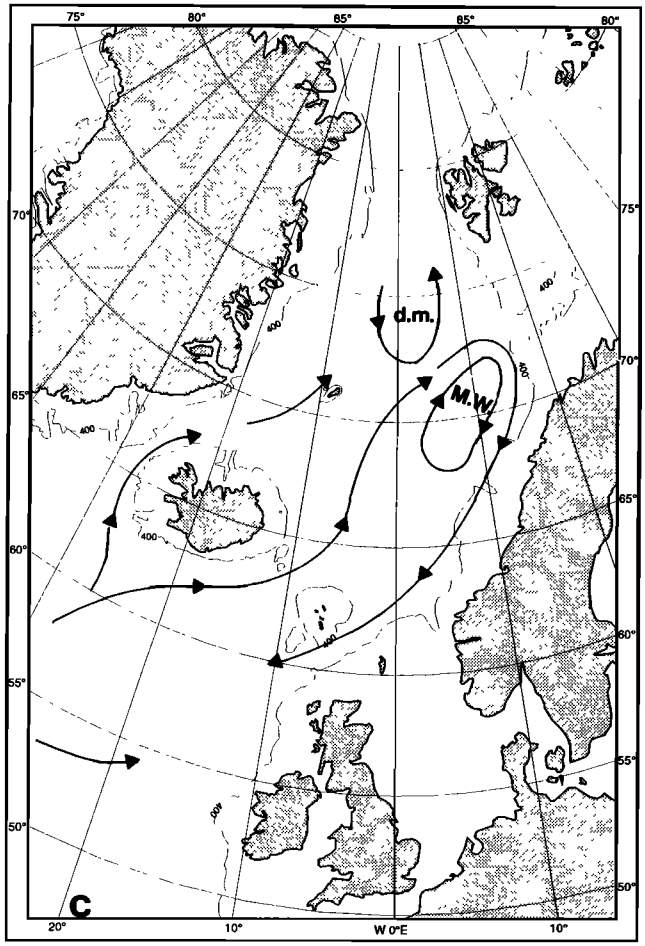

Figure 16. (continued)

directed warm-water transport in the northeast Atlantic and the southeastern Norwegian Sea (Figure 11c), and also by an extreme seasonality because of a closed sea ice cover during winter (Figure 12c) and a steep temperature gradient between the North Atlantic and the cold Norwegian Sea (Figure 12b). This evidence is in harmony with records of cold, maritime climates along the west coast of Norway and in Scotland, which indicate rapid ice advance down to the coast [*Sissons*, 1980; *Larsen et al.*, 1984]. Such an advance is consistent with a lowering of the glaciation limit by about 450 m, somewhat lower precipitation, a summer temperature reduction by about 8°C in west Norway [*Mangerud*, 1987; *Nesje*, 1992; A. Nesje, personal communication, 1993], and prevailing southwesterly winds in west Norway in the Younger Dryas [*Larsen et al.*, 1984].

On the other hand, the meridional character of North Atlantic circulation and the relatively warm temperatures off Ireland (Figure 12b) may contrast with the strong Younger Dryas cooling in Central and Western Europe, where there is evidence for both tundra and permafrost [*Larsen et al.*, 1984]. These contrasts perhaps may have resulted from both the extreme seasonality in the sea-ice cover of the Nordic Seas and persisting high pressure conditions over the widely glaciated North Europe, which led to prevailing cold northeasterly winds over central Europe. Onshore winds in this scenario would have been steered to the north of Central Europe, i.e., to the western flank of the Scandinavian peninsula.

Conclusions

Based on 110 age-calibrated planktonic $\delta^{18}O$ and $\delta^{13}C$ records of *Neogloboquadrina pachyderma* (s), combined with a number of planktonic foraminifer-based paleotemperature records, this study has reconstructed the regional distribution patterns of past surface-water masses in the northern North Atlantic (50-80°N). Regional variations in the reconstructed paleodensity patterns indicate that there were three major modes of surface-water circulation over the last 26,000 ^{14}C years (Figure 16).

1. The present Holocene-style circulation mode (Figure 16a) is dominated by meridional, cyclonic currents in the Nordic Seas and appears to be the most stable pattern, persisting over the last 12,800 ^{14}C years (including the Younger Dryas). Various meltwater incursions apparently did little to alter this circulation mode, such as incursions that originated from Norway in the late Bölling.

2. The peak glacial (LGM) circulation mode (Figure 16b) was stable over several thousand years, with cyclonic geostrophic currents in the at least seasonally ice-free Nordic Seas, similar to the Holocene circulation patterns. In the west, an enhanced paleo-Irminger Current entered the Icelandic Sea. In the east, however, the south-to-north advection of warm water across the eastern Iceland-Faeroe Ridge was barred, probably because of a long-lived meltwater lens west of Ireland. This lens may have resulted from iceberg flotillas that originated from the Laurentide ice sheet [*Robinson et al.*, 1995]. Dominant geostrophic forcing may have driven a sluggish clockwise rotation of the lens, thereby diverting the west-east advection of warm water away from West Europe, toward Iceland.

3. At the onset of the last deglaciation a great meltwater lens was produced by melting icebergs surging from the Barents Shelf ice. The lens led to a third circulation mode, with a small clockwise rotating gyre off Norway (Figure 16c). This mode only lasted for about 1000 years but induced a longshore flow of cold water (2°C in summer) as far south as Faeroe, which was compensated for by an enhanced paleo-Irminger inflow through the Denmark Strait.

Major North Atlantic meltwater masses, many of them related to Heinrich events [*Bond et al.*, 1992, 1993], have strongly influenced the northwest European climate over the last 80 kyr both by clockwise rotating current systems and via a turned-off or reduced heat advection by the salinity conveyor belt. A widespread meltwater lens west of Ireland, for example, chilled Western Europe over long parts of the LGM; a meltwater lens west of Norway led to the strong delay in climatic amelioration known as the Oldest Dryas cold spell. Generally, northeast Atlantic meltwater masses that were coeval with a strong reduction in summer insolation, such as during early stages 4 and 2, may have provided the missing trigger mechanism for abrupt buildups of continental ice sheets as yet unexplained by the gradual forcing of orbital cycles. No specific circulation mechanism, however, is found to explain the Younger Dryas cold spell; its $\delta^{18}O$ patterns depict a largely Holocene-style meridional circulation, and its low winter SSTs involve an extreme seasonality of sea ice cover.

Acknowledgments. We are grateful to D. Seidov for helping to interpret the paleocirculation, to R. Spielhagen for early insights into isotope data from the Arctic, to K. Winn for unpublished data of core 17045, and to many technicians and students that contributed with tedious but careful routine work to the large data set. We gratefully acknowledge the constructive comments and suggestions of anonymous reviewers and especially of Larry Peterson. This study re-

ceived generous support from the Sonderforschungsbereich 313 at Kiel University (publ. 212), the German National Program of Climate Research (07KF021), the Norwegian Research Council (POC-project), from the EU - ENVIRONMENT project, and the Centre National de la Recherche Scientifique, Institut National des Sciences de l'Univers, and Commissariat à l'Energie Atomique joint support to the Centre de Faibles Radioactivités, Gif-sur-Yvette.

References

Alm, T., Øvre Æråsvatn - palynostratigraphy of a 22,000 to 10,000 BP lacustrine record on Andøya, northern Norway, Boreas ,22, 171-188, 1993.

Andrieu, V., U. Eichler, and M. Reille, La fin du dernier Pléniglaciare dans les Pyrénées (France): Donnée polliniques, isotopiques et radiométriques, *C.R. Acad. Sci.* Ser. II, *316*, 245-250, 1993.

Bard, E., M. Arnold, J. Mangerud, M. Paterne, L. Labeyrie, J. Duprat, M.-A. Mélieres, E. Sonstegaard, and J.-C. Duplessy, The North Atlantic atmosphere-sea surface ^{14}C gradient during the Younger Dryas climatic event, *Earth Planet. Sci. Lett., 126*, 275-287, 1994.

Bard, E., B. Hamelin; R. G. Fairbanks, and A. Zindler, Calibration of the ^{14}C timescale over the past 30.000 years using mass spectrometric U-Th ages from Barbados corals, *Nature, 345*, 405-410, 1990.

Bauch, H., Planktische Foraminiferen im Europäischen Nordmeer - Ihre Bedeutung für die paläoozeanographische Interpretation während der letzten 600.000 Jahre, *Berichte Sonderforschungsbereich 313, 40,* 1-108, Univ. of Kiel, Kiel, Germany, 1993.

Becker, B., and B. Kromer, The continental tree-ring record - absolute chronology, ^{14}C calibration and climatic change at 11 ka, *Palaeogeogr. Palaeoclimatol. Palaeoecol. 103*, 67-72, 1993.

Beyer, I., Senkvartaer paleoseanografi i det sentrale Islandhav, M.Sc. thesis, 150 pp, Univ. of Bergen, Bergen, Norway, 1987.

Bischof, J. Dropstones im Europäischen Nordmeer. Ph. D. thesis, 127 pp., Univ. of Kiel, Kiel, Germany, 1990.

Bond, G., et al., Evidence for massive discharges of icebergs into the North Atlantic ocean during the last glacial period, *Nature, 360*, 245-249, 1992.

Bond, G., W. S. Broecker, S. Johnsen, J. McManus, L. Labeyrie, J. Jouzel, and G. Bonani, Correlations between climate records from North Atlantic sediments and Greenland ice, *Nature, 365*, 143-147, 1993.

Broecker, W.S., The strength of the nordic heat pump, in *The Last Deglaciation: Absolute and Radiocarbon Chronologies*, edited by E. Bard and W. S. Broecker; *NATO ASI-Ser., Ser. I, 2*, 173-182, 1992.

Broecker, W. S., and G. H. Denton, The role of ocean-atmosphere reorganizations in glacial cycles, *Geochim, Cosmochim. Acta, 53*(10), 2465-2501, 1989.

Broecker, W.S., and T.H. Peng, The oceanic salt pump: Does it contribute to the glacial-interglacial difference in atmospheric CO2 content?, *Global Biochemical Cycles, 3*, 215-239, 1989.

Broecker, W. S., D. M. Peteet, and D. Rind, Does the ocean - atmosphere system have more than one stable mode of operation?, *Nature, 315*, 21-26, 1985a.

Broecker, W. S., C. Rooth, and T. H. Peng, Ventilation of the deep northeastern Atlantic, *J. Geophys. Res., 90*, 6940-6944, 1985b.

Broecker, W.S., G. Bond, M. Klas, G. Bonani, and W. Wölfli, A salt oscillator in the Glacial Atlantic?, The concept, *Paleoceanography, 5*(4), 469-478, 1990.

Broecker, W.S. , G. Bond, K. Mieczyslawa, E. Clark, and J. McManus, Origin of the North Atlantic's Heinrich layers, *Clim. Dyn., 6*, 265-273, 1992.

Carstens, J., and G. Wefer, Recent distribution of planktonic foraminifera in the Nansen Basin, Arctic Ocean, *Deep-Sea Res..*, Part A, *39*, Suppl. 2, 507-524, 1992.

Charles, C. D., and R. G. Fairbanks, Evidence from Southern Ocean sediments for the effect of North Atlantic deepwater flux on climate, *Nature, 355*, 416-419, 1992.

Climate: Long Range Investigation, Mapping, and Prediction (CLIMAP), Seasonal reconstructions of the Earth'surface at the last glacial maximum, *GSA Map and Chart ser., MC-36*, Geol. Soc. of Am., Boulder, Color., 1981.

Cox, R.A., M.J. McCartney, and F. Culkin, The specific gravity /salinity / temperature relationship in natural seawater, *Deep-Sea Res., 17*, 679-689, 1970.

Curry, W. B., J.-C. Duplessy, L. D. Labeyrie, and N. J. Shackleton, Changes in the distribution of $\delta^{13}C$ of deep water • CO_2 between the last glaciation and the Holocene, *Paleoceanography, 3* (3), 317-341, 1988.

Dansgaard, W., et al., Evidence for general instability of past climate from a 250-kyr ice-core record, *Nature, 364*, 218-220, 1993.

Dietrich, G, and J. Ulrich, *Atlas zur Ozeanographie, Hochschulatlanten 307a-307m*, Bibiliographisches Institut, Mannheim, Germany, 1969.

Duplessy, J.-C., G. Delibrias, J. C. Turon, C. Pujol, and J. Duprat, Deglacial warming of the Northeastern Atlantic Ocean: Correlation with the paleoclimatic evolution of the European Continent, *Palaeogeogr. Palaeoclimatol. Palaeoecol., 35*, 121-144, 1981.

Duplessy, J.C., L. Labeyrie, A. Juillet-Leclerc, F. Maitre, J. Duprat, and M. Sarnthein, Surface salinity reconstruction of the North Atlantic Ocean during the last glacial maximum.- *Oceanol. Acta, 14*,(4), 311-324, 1991.

Duplessy, J.C., L. Labeyrie, M. Arnold, M. Paterne, J. Duprat, and T.C.E. Van Weering, Changes in surface salinity of the North Atlantic Ocean during the last deglaciation, *Nature, 358*, 485-487, 1992.

Elverhøi, A., W. Fjeldskaar,A. Solheim, M. Nyland-Berg, L. Russwurm, The Barents Sea ice sheet - A model of its growth and decay during the last ice maximum, *Quat. Sci. Rev., 12*, 863-873, 1992.

Emiliani, C., Rooth, C., and J.J. Stipp, The late Wisconsin Flood into the Gulf of Mexico, *Earth Planet. Sci. Lett. 41*, 159-162, 1978.

Eyles, N., and A. McCabe, The late Devensian (<22,000 BP) Irish Sea Basin: The sedimentary record of a collapsed ice sheet margin, *Quat. Sci. Rev., 8*, 307-352, 1989.

Fairbanks, R.G., A 17.000 year glacio-eustatic sea level record: Influence of glacial melting rates on the Younger Dryas event and deep-ocean circulation, *Nature, 143*, 637-642, 1989.

Fliri, F., S. Bortenschlager, H. Felber, W. Heissel, H. Hilscher, and W. Resch, Der Bänderton von Baumkirchen (Inntal, Tirol). Eine neue Schlüsselstelle zur Kenntnis der Würmvereisung der Alpen, *Z. Gletscherkd. Glazialgeol., 6*, 5-35, 1970.

Gordon, A.L., Interocean exchange of thermocline water, *J. Geophys. Res., 91*, 5037-5046, 1986.

Grousset, F. E., L. Labeyrie, J. A. Sinko, M. Cremer, G. Bond, J. Duprat, E. Cortijo, and S. Huon, Patterns of ice-rafted detritus in the glacial North Atlantic (40-55°N), *Paleoceanography, 8* (2), 175-192, 1993.

Hald, M., L.D. Labeyrie, D.A.R. Poole, P.I. Steinsund, and T.O. Vorren, Late Quaternary paleoceanography in the southern Barents Sea, *Nor. Geol. Tidsskr., 71*(3), 141-144, 1991.

Hebbeln D., T. Dokken, E. Anderson, M. Hald, and A.W. Elverhöi, Moisture supply for northern ice sheet growths during the last glacial maximum, *Nature, 370*, 357-360, 1994.

Henrich, R., *Beckenanalyse des Europäischen Nordmeeres: Pelagische und glaziomarine Sedimenteinflüsse im Zeitraum 2.6 Ma bis rezent,* Habilitationsschrift Math.-Nat. Fakultät, Univ. of Kiel, Kiel, Germany, 345 pp, 1992.

Horwege, S., Oberflächentemperaturen (und -Strömungen) der Norwegisch-Grönländischen See im Abbild stabiler Kohlenstoff- und Sauerstoffisotopen rezenter planktischer Foraminiferen, M.S. thesis, 47 pp., Univ. of Kiel, Kiel, Germany, 1987.

Hurdle, B. G., *The Nordic Seas*, 776 pp., Springer-Verlag, New York, 1986.

Imbrie, J., J.D. Hays, D.G. Martinson, A. McIntyre, A.C. Mix, J.J. Morley, N.G. Pisias, W.L. Prell, and N.J. Shackleton, The orbital theory of Pleistocene climate: Support from a revised chronology of the marine $\delta^{18}O$ record, in *Milankovitch and Climate*, edited by A. Berger et al., *NATO ASI Ser., Ser. C, 126*, 269-305, 1984.

Jansen, E., Rapid changes in the inflow of Atlantic water into the Norwegian Sea at the end of the last glaciation, in *Abrupt Climatic Change*, edited by W. H. Berger and L. D. Labeyrie, *NATO ASI Ser., Ser. I, 2*, 299-310, 1987.

Jansen, E., and T. Veum, Evidence for two-step deglaciation and its impact on North Atlantic deep water circulation, *Nature, 343*, 612-616, 1990.

Johannessen, T., E. Jansen, A. Flatöy, and A. C. Ravelo, The relationship between surface water masses, oceanic fronts and paleoclimatic proxies in surface sediments of the Greenland, Iceland, Norwegian Seas, in *Carbon Cycling in the Glacial Ocean: Constraints on the Ocean's Role in Global Change*, edited by R. Zahn, T.F. Pedersen, M.A. Kaminski, and L. D. Labeyrie, *NATO ASI Ser., Ser. I, 17*, 61-86, 1994.

Jones, G.A., and L. D. Keigwin, Evidence from Fram Strait (78°) for early deglaciation, *Nature, 336*, 56-59, 1989.

Joussaume, S., Simulations du climat du dernier maximum glaciaire a l'aide d'un modele de circulation generale de l'atmosphere incluant une modelisation de cycle des isotopes de l'eau et des poussieres d'origine desertique, Ph.D. thesis, 507 pp., Univ. P. et M. Curie, Paris, 507 pp., 1989.

Kaiser, K. F., *Beiträge zur Klimageschichte vom späten Hochglazial bis ins frühe Holozän, rekonstruiert mit Jahresringen und Molluskenschalen aus verschiedenen Vereisungsgebieten*, 203 pp., Eidgenöss. Forsch.anst. für Wald, Schnee und Landschaft, Birmensdorf, Switzerland, 1993.

Karpuz, N.K., and E. Jansen, A high resolution diatom record of the last deglaciation from the SE Norwegian Sea: Documentation of rapid climatic changes, *Paleoceanography, 7*(4), 499-520, 1992.

Keigwin, L.D., and E. A. Boyle, Late Quaternary paleochemistry of high-latitude surface waters, *Palaeogeogr. Palaeoclimatol. Palaeoecol., 3*, 85-106, 1989.

Keigwin, L.D., G.A. Jones, and S. J. Lehman, Deglacial meltwater discharge, North Atlantic deep circulation, and abrupt climate change, *J. Geophys. Res., 96*, 16,811-16,826, 1991.

Kellogg, T.B, Paleoclimatology and paleoceanography of the Norwegian Greenland seas: Glacial and interglacial contrasts, *Boreas, 9*, 115-137 1980.

Koc N., E. Jansen, and H. Haflidason, Paleoceanographic reconstructions of surface ocean conditions in the Greenland, Iceland and Norwegian Seas through the last 14ka: Based on diatoms, *Quat. Sci. Rev., 12*, 115-140, 1993.

Köhler, S.E.I., Spätquartäre paläo-ozeanographische Entwicklung des Nordpolarmeeres und Europäischen Nordmeeres anhand von Sauerstoff- und Kohlenstoffisotopenverhältnissen der planktischen Foraminifere *N. pachyderma* (sin.)., Ph.D. thesis, 104 pp., Univ. of Kiel, Kiel, Germany, 1991.

Koltermann, K. P., Die Tiefenzirkulation der Grönland-See als Folge des thermohalinen Systems des Europäischen Nordmeeres, Ph.D. thesis, 287 pp., Univ. of Hamburg, Hamburg, Germany, 1987.

Kromer, B., and B. Becker, German oak and pine ^{14}C calibration, 7200-9439 BC, *Radiocarbon, 35*, 125-135, 1993.

Labeyrie, L.D., and J.-C. Duplessy, Changes in the oceanic $^{13}C/^{12}C$ ratio during the last 140,000 years: High latitude surface water records, *Palaeogeogr. Palaeoclimatol, Palaeoecol., 50*, 217-240, 1985.

Labeyrie, L.D., J.C. Duplessy, J. Duprat, A. Juillet-Leclerc, J. Moyes, E. Michel, N. Kallel, and N. Shackleton, Changes in the vertical structure of the North Atlantic Ocean between glacial and modern times, *Quat. Sci. Rev., 11*, 401-414, 1992.

Lackschewitz, K.S. , Sedimentationsprozesse am aktiven mittelozeanischen Kolbeinsey Rücken (nördlich von Island), Ph.D. thesis, 121 pp., Univ. of Kiel, Kiel, Germany, 1991.

Lamb, H.H., Climate present, past and future, *Climatic History and the Future*, vol. 2, 835 pp., (Methuen, New York), 1977.

Landvik, J. Y., M. Bolstad, A.K. Lycke, J. Mangerud, and H. P. Sejrup, Weichselian Stratigraphy and palaeoenvironments at Bellsund, western Svalbard, *Boreas, 21*, 335-358, 1992.

Larsen, E., F. Eide, O. Longva, and J. Mangerud, Alleröd-Younger Dryas climatic inferences from cirque glaciers and vegetational development in the Nordfjord Area, western Norway, *Arct. and Alp. Res., 16*, 137-160, 1984.

Larsen, E., S. Gulliksen, S.-E. Lauritzen, R. Lie, R. Løvlie, and J. Mangerud, Cave stratigraphy in western Norway: Multiple Weichselian glaciations and interstadial vertebrate fauna, *Boreas, 16*, 267-292, 1987.

Lautenschlager, M., Simulations of the ice age atmosphere - January and July means, *Geol. Rundsch., 80*, 513-534, 1991.

Lehman, S., and L. D. Keigwin, Sudden changes in North Atlantic circulation during the last deglaciation, *Nature, 356*, 757-762, 1992.

Lehman, S., G.A. Jones, L.D. Keigwin, , E.S. Andersen, G. Butenko, and S.-R. Ostmo, Initiation of Fennoscandian ice-sheet retreat during the last glaciation, *Nature, 349*, 513-516, 1991.

Leuenberger, M, U. Siegenthaler, and C. C. Langway, Ice -age $\delta^{13}C$ of atmospheric CO_2 from an Antarctic ice core, *Nature, 357*, 488-490, 1992.

Lotter, A.F., J. Beer, I. Hajdas, and M. Sturm, A step towards an absolute time-scale for the Late-Glacial: Annually laminated sediments from Soppensee (Switzerland), in *The Last Deglaciation: Absolute and Radiocarbon Chronologies*, edited by E. Bard and W. S. Broecker; *NATO ASI Ser., Ser. I, 2*, 45-68, 1992.

MacAyeal, D.R., Binge/purge oscillations of the Laurentide ice sheet as a cause of the North Atlantic's Heinrich events, *Paleoceanography*, 8(6), 775-784, 1993.

Manabe, S. and A.J. Broccoli, The influence of continental ice sheets on the climate of an ice age, *J. Geophys. Res., 90*, 2167-2190, 1985.

Mangerud, J., The Alleröd/Younger Dryas boundary, in *Abrupt Climatic change*, edited by W.H. Berger and L.D. Labeyrie, pp. 163-171, *NATO ASI Ser., Ser. I, 2*, 1987.

Mangerud, J. The last interglacial/glacial cycle in Northern Europe, in *Quaternary Landscapes*, edited by Shane, L.C.K. and E.J. Cushing (eds.), 38-75, Univ. of Minn. Press, Minneapolis, 1991.

Mangerud, J., and J.I. Svendsen, The last interglacial-glacial period on Spitsbergen, Svalbard, *Quat. Sci. Rev., 11*, 633-664, 1992.

Mangerud, J., S.E. Lie, H. Furnes, I.L. Kristiansen, and L. Lömo, A Younger Dryas ash bed in western Norway and its possible correlations with tephra in cores from the Norwegian Sea and the North Atlantic, *Quat. Res., 21*, 85-104, 1984.

Nesje, A., Younger Dryas and Holocene glacier fluctuations and equilibrium-line altitude variations in the Jostedalsbre region, western Norway, *Clim. Dyn., 6*, 221-227, 1992.

Olausson, E., Oceanographic aspects of the Pleistocene of the Arctic Ocean, *Inter-Nord, 12*, 151-170, 1972.

Oppo, D., and R. G. Fairbanks, Mid-depth circulation of the subpolar North Atlantic during the last glacial maximum, *Science, 259*, 1148-1152, 1993.

Paus, A., Late Weichselian vegetation, climate and floral migration at Liastemmen, North Rogaland, south-western Norway, *J. Quat. Sci., 4*, 223-242, 1989.

Paus, A., Late Weichselian and early Holocene vegetation, climate, and floral migration at Utsira, North Rogaland, south-western Norway, *Nor. Geol. Tidsskr. 70*, 135-152, 1990.

Pflaumann, U., J. Duprat, C. Pujol, and L.D. Labeyrie, SIMMAX, a transfer technique to deduce Atlantic sea surface temperatures from planktonic foraminifera - the EPOCH approach, *Paleoceanography*, 1995 (in press).

Pflaumann, U., and H. Hensch, Paleoceanography of the Norwegian and East Greenland Margins: Temperature transfer functions, in *Nordatlantik 1993 Cruise No. 26*, edited by E. Suess, K. Kremling, and J. Mienert, pp. 74-101, Leitstelle METEOR, Univ. of Hamburg, Hamburg, Germany, 1994.

Robinson, S.G., M.A. Maslin, and N. McCave, Magnetic susceptibility variations in Late Pleistocene deep-sea sediments of the northeast Atlantic: Implications for ice rafting and paleocirculation at the last glacial maximum, *Paleoceanography*, 10(2), 221-250, 1995.

Rooth, C., Hydrology and ocean circulation, *Progr. in Oceanogr., 7*, 131-149, 1982.

Rosell-Melé, A., Long-chain alkenones, alkyl alkenoates and total pigment abundance in the north eastern Atlantic, Ph.D. thesis, Univ. of Bristol, Bristol, England, 1994.

Ruddiman, W. F., and A. McIntyre, The North Atlantic Ocean during the last deglaciation, *Palaeogeogr. Palaeoclimatol. Palaeoecol., 35*, 145-214, 1981.

Sarnthein, M., E. Jansen, J.-C. Duplessy, H. Erlenkeuser, A. Flatøy, T. Veum, E. Vogelsang, and M. Weinelt, $\delta^{18}O$ time-slice reconstruction of meltwater anomalies at Termination I in the North Atlantic between 50 and 80°N, in *The Last Deglaciation: Absolute and Radiocarbon Chronologies*, edited by E. Bard and W. S. Broecker; *NATO ASI Ser., Ser. I, 2*, 183-200, 1992.

Sarnthein, M. , K. Winn, S. J. A. Jung, J. C. Duplessy, L. D. Labeyrie, H. Erlenkeuser, and G. Ganssen, Changes in East Atlantic Deep Water Circulation over the last 30,000 Years: An eight time-slice record, *Paleoceanography, 9(2)*, 1994.

Schäfer-Neth, C.,Modellierung der Paläoozeanographie des nördlichen Nordatlantiks zur letzten Maximalvereisung, Ph.D. thesis, pp. 1-106, Univ. of Kiel, Kiel, Germany, 1994.

Schulz, H., Meeresoberflächentemperaturen im Nordatlantik und in der Norwegisch-Grönländischen See vor 9.000 Jahren. Auswirkungen des frühholozänen Insolationsmaximums, Ph.D. thesis, pp. 1-119, Univ. of Kiel, Kiel, Germany, 1994.

Sejrup, H.P., H. Haflidason, I. Aarseth, E. King, C.F. Forsbeck, D. Long, and K. Rokoengen, Late Weichselian glaciation history of the northern North Sea, *Boreas, 23*, 1-13, 1994.

Shackleton, N.J., J. Imbrie, and M. A. Hall, Oxygen and carbon isotope record of the East Pacific core V19-30: Implications for the formation of deep water in the late Pleistocene North Atlantic, *Earth Planet. Sci. Lett., 65*, 233-244, 1983.

Shackleton, N.J., and N. G. Pisias, Atmospheric carbon dioxide, orbital forcing, and climate, in *The carbon cycle and Atmospheric CO_2: Natural Variations Archean to Present, Geophys. Monogr. Ser., Vol. 32*, pp. 303-317, edited by E.T. Sunquist and W.S. Broecker, AGU, Washington, D.C., 1985.

Sissons, B., Paleoclimatic inferences from from Loch Lomond advance glaciers, in *Late Glacial of North-West Europe*, edited by J.J. Lowe, J.M. Gray, and J.E. Robinson, pp. 31-43, Pergamon, Tarrytown, N.Y., 1980.

Spielhagen, R. F., and H. Erlenkeuser, Stable oxygen and carbon isotopes in planktic foraminifers from Arctic Ocean surface sediments: Reflection of the low salinity surface water, *Mar. Geol., 119*, 227-250, 1994.

Stein, R., C. Schubert, C. Vogt, and D. Fütterer, Stable isotope stratigraphy, sedimentation rates, and salinity changes in the latest Pleistocene to Holocene eastern central Arctic Ocean, *Mar. Geol., 119*, 333-356, 1994.

Steinsund, P.I., M. Hald, and D. Poole, Modern benthic foraminiferal distribution in the southwestern Barents Sea, *Nor. Geol. Tidsskr., 3*, 169-171, 1991.

Stommel, H., Thermohaline convection with two stable regimes of flow, *Tellus, 13*, 224-230, 1961.

Struck, U., Zur Paläo-Ökologie benthischer Foraminiferen im Europäischen Nordmeer während der letzten 600 000 Jahre, Ph.D. thesis, 89 pp., Univ. of Kiel, Kiel, Germany, 1992.

Struck, U., and S. Nees, Die stratigraphische Verbreitung von *Siphotextularia rolshauseni* (PHLEGER & PARKER) in Sedimentkernen aus dem Europäischen Nordmeer, *Geol. Jahrb., Reihe A, 128*, 243-249, 1991.

Taylor, K. C., G. W. Lamorey, G. A. Doyle, R. B., Alley, P. M. Grootes, P. A. Mayewski, J. W. C. White, and L. K. Barlow, The 'flickering switch' of late Pleistocene climate change, *Nature, 361*, 432-436, 1993.

Veum, T., E. Jansen, M. Arnold, I. Beyer, and J.-C. Duplessy, Water mass exchange between the North Atlantic and the Norwegian Sea during the last 28.000 years, *Nature, 356*, 783-785, 1992.

Vogelsang, E., Paläo-Ozeanographie des Europäischen Nordmeeres an Hand stabiler Kohlenstoff- und Sauerstoffisotopen, Ph.D. thesis, 136 pp., Univ. of Kiel, Kiel, Germany, 1990.

Vorren, T.O., and Y. Kristoffersen, Late Quaternary glaciation in the southwestern Barents Sea, *Boreas, 15*, 51-59, 1986.

Vorren, T., K.-D. Vorren, T. Alm, S. Gulliksen and R. Løvlie, The last deglaciation (20,000-11,000 B.P.) on Andøya, northern Norway, *Boreas 17*, 41-77, 1988.

Weinelt, M., Veränderungen der Oberflächenzirkulation im Europäischen Nordmeer während der letzten 60.000 Jahre - Hinweise aus stabilen Isotopen, Ph.D. thesis, 105 pp., Univ. of Kiel, Kiel, Germany, 1993.

Weinelt, M., M. Sarnthein, E. Vogelsang, and H. Erlenkeuser, Early decay of the Barents Shelf Ice Sheet. Spread of stable isotope signals across the Norwegian Sea, *Nor. Geol. Tidsskr., 71*(3), 137-140, 1991.

Weinelt, M., M. Sarnthein, H. Schulz, and S. Jung, Ice-free Nordic Seas during the last Glacial Maximum? - Potential sites of deepwater formation, *Paleoclimates, Data and Modelling*, in press, 1996.

Winn, K., M. Sarnthein, and H. Erlenkeuser, $\delta^{18}O$ stratigraphy and chronology of Kiel sediment cores from the East Atlantic, *Ber.-Rep., 45*, 1-99, Geol.-Paläont. Inst. Univ. Kiel, Kiel, Germany, 1991.

Wold, C., Paleobathymetry and sediment accumulation in the northern North Atlantic and southern Greenland-Iceland-Norwegian Sea, Ph.D. thesis, pp. 1-255, Univ. of Kiel, Kiel, Germany, 1992.

Zahn, R., B. Markussen, and J. Thiede, Stable isotope data and depositional environments in the late Quaternary Arctic Ocean, *Nature, 314*, 433-435, 1985.

M. Arnold, J.C. Duplessy, and L. Labeyrie, Centre des Faibles Radioactivités, F-91198 Gif sur Yvette CEDEX, France

H. Erlenkeuser, Leibniz Labor für Altersbestimmung und Isotopenforschung, University of Kiel, Olshausenstrasse 40, D-24098 Kiel Germany.

A. Flatøy, E. Jansen, G. Johannessen, T. Johannessen, and Nalan Koc, Department of Geology, University of Bergen, Allégatan 41, N-5007 Bergen, Norway.

S. Jung, M. Maslin, U. Pflaumann, M. Sarnthein, H. Schulz, and M. Weinelt, Geologisch-Paläontologisches Institut, University of Kiel, Olshausenstrasse 40, D-24098 Kiel Germany. (e-mail: ms@gpi.uni-kiel.de)

(Received April 4, 1994; revised May 3, 1995; accepted May 4, 1995.)